Journal of Cleaner Production 330 (2022) 129529

Contents lists available at ScienceDirect

Journal of Cleaner Production

journal homepage: www.elsevier.com/locate/jclepro

Acid/base flow battery environmental and economic performance based on its potential service to renewables support

Maryori C. Díaz-Ramírez [a,b,*], Maria Blecua-de-Pedro [a], Alvaro J. Arnal [a], Jan Post [c]

[a] Research Centre for Energy Resources and Consumption (CIRCE). Avenida Ranillas, Edificio Dinamiza, 3D, 50018, Zaragoza, Spain
[b] Instituto Universitario de Investigación CIRCE, Fundación CIRCE, Universidad de Zaragoza, 50009, Zaragoza, Spain
[c] Wetsus, European Centre of Excellence for Sustainable Water Technology, 8911, MA, Leeuwarden, Netherlands

ARTICLE INFO

Handling Editor: Zhifu Mi

Keywords:
Energy storage
Acid base flow battery
Vanadium redox flow battery
Life cycle assessment
Life cycle cost
Environmental indicators

ABSTRACT

An innovative technology, called Acid Base Flow Battery (AB-FB), has been developed to overcome the intermittent supply of wind and solar electricity generation. It stores electrical energy using pH and salinity differences in the water and compared with other battery technologies, such as Vanadium Redox Flow Battery (VRFB), the new system is expected to be safer, more sustainable and to become a cost competitive option. To provide a deeper knowledge of the new system potentials, in this research, Life Cycle studies under cradle to grave approach have been carried out to assess the environmental and economic performance of 1 MW/6 MWh AB-FB system. Furthermore, 1 MW/6 MWh VRFB has been considered as the reference case. According to the comparative analysis, the AB-FB system exhibited the best environmental and economic performance, placing the AB-FB system as the most sustainable technology. In terms of environmental impacts related to the three process stages, the AB-FB system operation stage yielded the most relevant environmental burden, mostly attributed to energy losses due to the system efficiency. Manufacturing of the AB-FB system was the second stage with the more significant quote to the total environmental burden. Particularly, impacts were related to the power subsystem components being steel, copper, polyethylene and polyvinylchloride identified as the key materials responsible of this tendency. In contrast, the VRFB manufacturing was the most relevant process stage in terms of environmental implications. The energy subsystem was responsible for this tendency due to the vanadium-based electrolyte production related impacts. This component of the VRFB system was also its main constrains in terms of costs. The VRFB investment cost (339 €/kWh) was almost twice the AB-FB one (184 €/kWh), mostly affected by the VRFB electrolyte cost production.

1. Introduction

Among all the current battery approaches, flow batteries represent one of the most promising technologies to overcome electricity supply limitations in the renewable energy market (Sánchez-Díez et al., 2021). In fact, Vanadium Redox Flow Batteries (VRFB) have risen as one of the most emerging technologies to effectively store renewable energy (Díaz-Ramírez et al., 2020a, 2020b; Lourenssen et al., 2019; Weber et al., 2018). This technology seems to fulfil criteria, such as safety, durability, economic competitiveness, and site-independence. Besides, it offers independent scalability of its power and energy capacity, deep discharge capacity and a cycle life suitable for solar PV power applications (Bhattacharjee et al., 2018). All of these characteristics are considerably advantageous for the VRFB technology, especially when acts as Renewable Energies Support (RES). However, some environmental issues related to the components of the battery can be also identified (Díaz-Ramírez et al., 2020b).

Vanadium, which is the based on the VRFB electrolyte, has been recently listed as a Critical Raw Material (CRM) (European Commission, 2020a). The consumption of this resource constitutes a challenge for this type of Energy Storage System (ESS) in the near future, especially in the frame of the industry 5.0 (European Commision, 2021). In addition, the vanadium-based electrolyte production cost is mostly responsible for the high cost of the VRFB technology compared with other ESS technologies use as RES, such as lithium ion batteries or pumped hydro storage (Coester et al., 2020; Javed et al., 2021; Li et al., 2017; Lourenssen et al., 2019; Noack et al., 2016). On the other hand, VRFB electrolyte is made of sulfuric acid which may cause degradation within the cell lowering the battery life (Lourenssen et al., 2019).

* Corresponding author. Research Centre for Energy Resources and Consumption (CIRCE). Avenida Ranillas, Edificio Dinamiza, 3D, 50018, Zaragoza, Spain.
E-mail address: maryoried28@gmail.com (M.C. Díaz-Ramírez).

https://doi.org/10.1016/j.jclepro.2021.129529
Received 5 May 2021; Received in revised form 13 September 2021; Accepted 27 October 2021
Available online 31 October 2021

Nomenclature

AB-FB	Acid Base Flow Battery
APOS	Allocation at the point of substitution
AEM	Anion Exchange Membrane
C_{EE},a	Annualized External Environmental Cost
C_{DR},a	Annualized Disposal and Recycling Cost
CR,a	Annualized Future Cost of Replacement
C_{LCC},a	Annualized Life Cycling Costs
$C_{O\&M}$,a	Annualized Operation & Maintenance costs
Ccap,a	Annualized Total Capital Cost
BOP	Balance of Plant
BMS	Battery Management System
BPM	Bipolar Membrane
BPMED	Bipolar Membrane Electrodialysis
BPMRED	Bipolar Membrane Reverse Electrodialysis
CAPEX	Capital Expenditure,
CEM	Cation Exchange Membrane
CRM	Critical Raw Material
CRF	Capital Recovery Factor
DoD	Depth of Discharge
CDR,a	Disposal and Recycling Costs
EoL	End-of-Life
ESS	Energy Storage System
EI	Environmental Indicator
ELCC	Environmental Life Cycle Cost
ECF	External Cost Factor
C_{EE}	External Environmental Cost
PMFP	Fine Particulate Matter Formation
FFP	Fossil Resource Scarcity
FETP	Freshwater Ecotoxicity
FEP	Freshwater Eutrophication
FC	Fuel Cell
FU	Functional Unit
GWP	Global Warming Potential
HTPc	Human Carcinogenic Toxicity
HTPnc	Human Non-Carcinogenic Toxicity
IRP	Ionizing Radiation
LOP	Land Use
LCOE	Levelized Cost of Electricity
LCC	Life Cycle Cost
LCA	Life Cycle Analysis or Assessment
LCI	Life Cycle Inventory
LDPE	Low Density Polyethylene
METP	Marine Ecotoxicity
MEP	Marine Eutrophication
SOP	Mineral Resource Scarcity
LCOS	Net Levelized Cost Of Storage
ηsys	Overall Efficiency
HOFP	Ozone Formation, Human Health
EOFP	Ozone Formation, Terrestrial Ecosystems
PV	Photovoltaic Panels
PE	Polyethylene
PP	Polypropylene
PCS	Power Conversion System
RFB	Redox Flow Batteries
RS	Renewable Energy Sources Support
REDOX	Reduction-Oxidation Reactions
RTE	Round Trip Efficiency
SoC	State of charge
ODP	Stratospheric Ozone Depletion
SMES	Superconducting Magnetic Energy Storage
SI	Supporting Information
TAP	Terrestrial Acidification
Tetp	Terrestrial Ecotoxicity
TCC	Total Capital Cost
VR	Valve Regulated
Vrfb	Vanadium Redox Flow Battery
WCP	Water Consumption
WT	Wind Turbines

By considering these constraints, a potentially more sustainable flow battery is the so-called Acid Base Flow Battery (AB-FB). This innovative technology is based on the reversible water dissociation by bipolar membranes, and it stores electricity in the form of chemical energy in acid and base solutions (Culcasi et al., 2020; Pärnamäe et al., 2020). A schematic representation of the AB-FB is depicted in Fig. 1. In particular, the Bipolar Membrane Electrodialysis (BPMED) process uses electrical energy to produce acidic and alkaline solutions that are then exploited in the reverse process, i.e. the Bipolar Membrane Reverse Electrodialysis (BPMRED) to generate electricity (Culcasi et al., 2020).

This technology is foreseen to be attractive for stationary electrical energy storage and might offer scalability (kWh up to MW-MWh) suitable for different capacities and applications. The risks of the AB-FB system are extremely low, as the system cannot be overcharged or over-discharged, the salt solutions and the electrodes are thermally stable, no exothermic reactions are involved and hence, there is no risk of a thermal runaway.

In contrast with the VRFB technology, the new system is composed by an electrolytic solution based on water and salt. It does neither contain toxic chemicals nor scarce elements, which might result into a safer and more sustainable technology than other commercially available batteries (van Egmond et al., 2018). Furthermore, the AB-FB technology exhibits minimal issues of degradation and contamination since salt composition is kept without interactions with other elements. Finally, in terms of costs, the AB-FB system has the potential to achieve very low capital cost levels per kWh storage (Culcasi et al., 2020). In fact, the capital cost levels per kW are mostly dependent on components such as membranes and stacks, which are still under development (Pärnamäe et al., 2020).

According to the state of the art of literature, a similar approach to the AB-FB system has been recently published (Morales-Mora et al., 2021). There is, however, no evidence how the system would perform in practice. Furthermore, compared to the AB-FB system, some limitations can be anticipated. On the one hand, it has been applied a high salt concentration (1.6M) (Morales-Mora et al., 2021), which is foreseen as one drawback of the membrane selectivity (Fan and Yip, 2019). Moreover, contrary to previously mentioned experimental work on the AB-FB technology (van Egmond et al., 2018), Na_2SO_4 has been considered instead of NaCl as electrolyte (Morales-Mora et al., 2021). It might cause environmental implications due to the formation of electrolyte components such as H_2SO_4 (Morales-Mora et al., 2021). Effects of this type of component have been reported to the VRFB system in literature (Díaz-Ramírez et al., 2020b; Weber et al., 2018).

In order to gain more insight into the aforementioned AB-FB expected potentials, it is needed to carry out a detailed evaluation of the environmental and economic potential of the innovative technology. Many authors studied and compared applicability of ESS through the Life Cycle approach (Gouveia et al., 2020b; Longo et al., 2013; Zhang et al., 2020). This methodology is the most widely used to evaluate the product or system related impacts through its life cycle, which implies

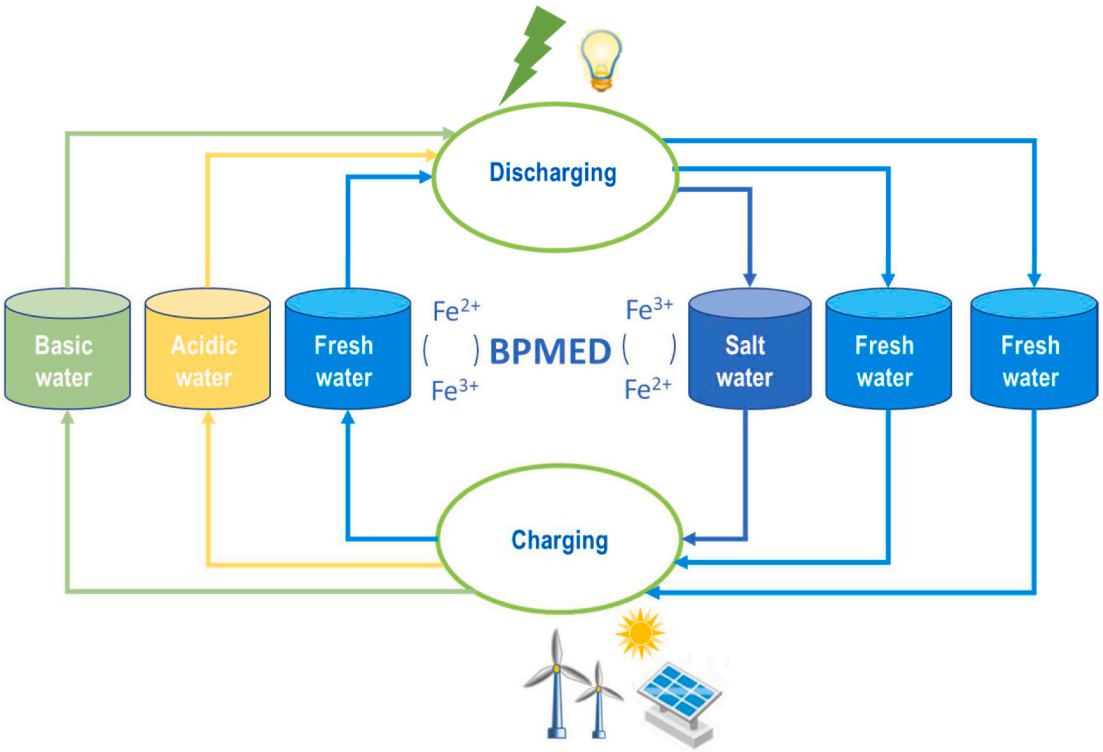

Fig. 1. Schematic representations of the AB-FB system. Adapted from (Culcasi et al., 2020).

all production stages from the extraction and processing of the raw materials to the final disposal of the product. Particularly, the environmental impacts are evaluated by applying Life Cycle Assessment (LCA) studies (Lopez et al., 2020; Morales-Mora et al., 2021; Weber et al., 2018) whereas economic issues can be revised by performing Life Cycle Cost analysis (Battke et al., 2013; Zakeri and Syri, 2015).

Under this premise, the specific objectives of this work were:

i) To generate an exhaustive analysis of the AB-FB environmental performance from the point of view of the LCA studies to identify environmental hotspots and potential measures to improve the environmental behaviour of the AB-FB system,
ii) To develop a revision of the AB-FB system applicability for RS by assessing different operation scenarios in terms of energy source for electricity generation and origin with the aim of exploring conditions fostering a more ESS sustainable service,
iii) To perform an analysis of related costs attributed to the life cycle of the AB-FB technology to determine the most influential financial aspects.

Life cycle approaches were applied in this work to generate valuable and more quantitative information concerning environmental and economic performance of the AB-FB technology. Information generated from these studies will be also compared with the one obtained to the VRFB system, which was considered for benchmarking purposes, by following same methodological approaches.

Results attained by this research were aimed to not only update the state of the art of batteries as energy storage units but also to provide a deeper knowledge on potential impacts of the new technology. Based on this study, possible applications and needs for further development of the new AB-FB technology have been identified, and potentials to become a competitor of VRFB in terms of environmental as well as economy issues have been explored.

2. Materials and methods

In this section, the two-battery cases are introduced, and a detailed description of the evaluation methodology is presented.

The methodological approach considered in this work was primarily focused on gaining a deeper understanding of the environmental and economic performance of 1 MW/6 MWh AB-FB system. To carry out this type of evaluation, Life Cycle studies have been developed to the new technology from a Cradle to Grave approach. Secondly, it was done a comparative evaluation of the AB-FB system results with the ones generated to the VRFB system (benchmarking technology). To guarantee comparison of the results, raw data gathered to the VRFB was processed by following the LCA/LCC methodological approaches applied to the AB-FB system. Finally, a sensitivity study was performed for evaluating the influence of the different battery operation parameters.

2.1. Battery study cases

The two battery systems analysed in this paper were characterised by a mean power of 1 MW and, particularly, a nominal capacity of 9.7 MWh for the AB-FB system and 8.3 MWh for the VRFB system.

The innovative AB-FB technology is composed of three main subsystems:

i) Power subsystem or stack (determining the power rating), where many membranes are stacked in a repetitive manner named triplet-cells and also called the reaction units of the AB-FB system. One triplet-cell is constituted by three membranes: one Cationic Exchange Membrane (CEM), one Anionic Exchange Membrane (AEM) and one Bipolar Membrane (BPM), consisting of CEM and AEM.
ii) Energy subsystem (determining the storage capacity), which comprises the aqueous salt and electrolyte (where the chemical energy is stored) solutions as well as the associated components for storage.

iii) Periphery, which corresponds to pumps, pipes, inverter, battery management system and Process Control System (PCS).

Similarly, to the AB-FB system, the VRFB technology is divided into three main subsystems (Weber et al., 2018):

i) a power subsystem comprising all components related with the stack and the battery cells (determining the power rating).
ii) an energy subsystem constituted by the electrolyte and associated components (determining the storage capacity).
iii) all remaining components are assigned to be the periphery: one heat exchanger, the inverter, BMS and PCS.

A summary of the main technical parameters related to these two technologies is included in Table 1. The design parameters of the AB-FB system were obtained from the development path envisioned by the BAoBaB project (www.baobabproject.eu) for 2025 (Pärnamäe et al., 2020). For VRFB, the design parameters were obtained from the literature (Weber et al., 2018). In both cases, the effective energy capacity corresponded to 6 MWh (see Table 1), as this parameter depended on the application. For comparative reasons, the AB-FB system described here was thought to work in same applications as the VRFB system. For this reason, the final specifications of the AB-FB system were a power capacity of 1 MW and a net storage capacity 6 MWh.

Effective capacity (Ce) was quantified by multiplying nominal capacity (Cn) by the Round Trip Efficiency (RTE), also named energy efficiency, and the Depth of Discharge (DoD), according to equation (1):

$$Ce\ (MWh\ provided) = Cn\ \times RTE \times DoD \quad (1)$$

Based on the future scenario for 2025 (Pärnamäe et al., 2020), the AB-FB power density would be 41.75 W/m^2 of membrane (or 125 W/m^2 of triplet), and the RTE equal to 65%. This power density is 3 times higher than the current one when working with the available membranes (30–40 W/m^2 per triplet) (Pärnamäe et al., 2020). However, it is three times lower than values projected in a bipolar electrodialysis flow battery study (335 W/m^2 per triplet) (Morales-Mora et al., 2021). The value selected in the current study has been chosen under an optimistic and successful development system with thinner membranes and lower internal resistance expected to be available in the future.

In the case of the RTE, the selected value (65%) is closely achievable with the current membranes (up to 63%), depending on the battery design and operation (Pärnamäe et al., 2020). Morales-Mora et al. (2021) selected a RTE efficiency equal to 75%, which probably related to a very optimistic scenario (Morales-Mora et al., 2021). A lower value has been selected in this study in order to reflect the membrane selectivity loss over the battery life due to the energy expenditure during the electrolyte regeneration.

For the sake of this study, another important assumption has been to consider a cycle life of 10,000 over a calendar life of 10 years, which is not proven yet. The current BPM would be expected to lose functionality much sooner, especially due to the constant and cyclic water swelling at the interphase. However, an improvement of the BM cyclability has been one of the key targets of the BAoBaB project, leading to an optimistic opinion regarding this parameter.

Table 1
Technical data of batteries.

Design parameters	Unit	AB-FB (BAoBaB project)	VRFB (Weber et al., 2018, paper and SI)
Specific energy	Wh/kg	3.25	19.4
Cycle life	Cycles	10000	10000
Lifetime (defined to the system dismantling)	years	20	20
Rated power or power capacity	MW	1	1
Design capacity or nominal capacity	MWh	9.7	8.3
Discharge time	h	9.7	8.3
Effective energy capacity or net storage capacity	MWh	6	6
Reverse cell voltage	V	0.83	1.35
Number of triplet-cells	–	8064	155
Number of stacks	–	36	2
Membrane surface per cell	m^2	0.99	3.87
Power density	W/m^2	41.75	833.54
Round Trip Efficiency (RTE) or Energy efficiency	%	65	75
Depth of Discharge (DoD)	%	95	95
Min SoC	%	5	5
Replacement power subsystem	–	every 10 years	every 10 years

2.1.1. AB-FB (innovative technology)

As it was introduced in previous section, the assessed system corresponds to a mean power of 1 MW and effective energy capacity of 6 MWh. For a nominal power of 1 MW, 36 stacks, with 224 triplet-cells each (8064 in total), are required. The stack is an assembly of a certain number of triplet-cells, which are made of three membrane types: AEM, BPM and CEM. A simplified representation of the stack assembly is depicted in Fig. 2. Between the membranes, spacer-filled gaskets are placed creating a place for the solutions. 16 times 14 triplets are piled between divider plates and endplates. The endplates contain carbon felt electrodes connected to the current collectors. The stacks are contained between steel plates, tightened together by steel rods.

To reach the effective energy capacity of 6 MWh, an electrolyte volume of 1846 m^3 is required. This volume is divided over three equally sized reservoirs (acid/base/salt, see Fig. 2), with a starting sodium chloride concentration of 1.0 mol/l. An electrode rinse solution of 1.0 mol/l $FeCl_2$ and $FeCl_3$ is contained in an 8 m^3 LDPE tank, with its corresponding pump. Each of the acid/base/salt circuits requires two centrifugal pumps. Pipes with a length of 100 m from the reservoirs to the cells are required too.

The AB-FB system energy is stored in both, salinity, and pH gradients. These gradients are constituted by the separation of ions from acid, base and salt (or water) solutions. In this way, this system counts with four types of solutions: HCl (aq), NaOH (aq), H_2O and NaCl (aq). The separation of ions is done similarly to the well-known BPMED during charging reactions, while energy is storage and BPMRED during discharging reactions while power generation occurs (Culcasi et al., 2020; Pärnamäe et al., 2020; van Egmond et al., 2018).

As it is summarised in Fig. 3, during charging process, fresh water is pumped to the compartments adjacent to the BPM, and at the BPM junction water separates into OH^- and H^+ ions due to the supplied electrical energy. From the salt solution, the CEM supplies the Na^+ counterion for the OH^-, and the AEM the Cl^- counterion for the H^+. Hence, OH^- and Na^+ ions are combined and stored as dissolved NaOH (basic solution), while H^+ and Cl^- ions undergone the same process to be stored as dissolved HCl (acidic solution). At the same time, reversible reduction-oxidation reactions occur at the electrodes. Reduction of Fe (III) takes place at the one electrode acting as a cathode (Fe^{3+} (aq) + e^- -> Fe^{2+} (aq)), and oxidation of Fe(II) at the other acting as an anode (Fe^{2+} (aq) -> Fe^{3+} (aq) + e^-), fed by the external circuit of the battery.

During the discharge process, the opposite reactions occur. Electrical energy is recovered from neutralizing the acidic and basic solutions at the bipolar junction inside the BPM, to finally recombine the H^+ and OH^- to water, and the Na^+ and Cl^- to a NaCl solution. Reversed to the charging processes, at the one electrode Fe(II) is oxidized (i.e., the electrode now acts as anode), whereas at the other Fe(III) becomes reduced (i.e., the electrode now acts as cathode). A deeper explanation about the technology behind this battery can be found in the literature (Culcasi et al., 2020; Pärnamäe et al., 2020; van Egmond et al., 2018).

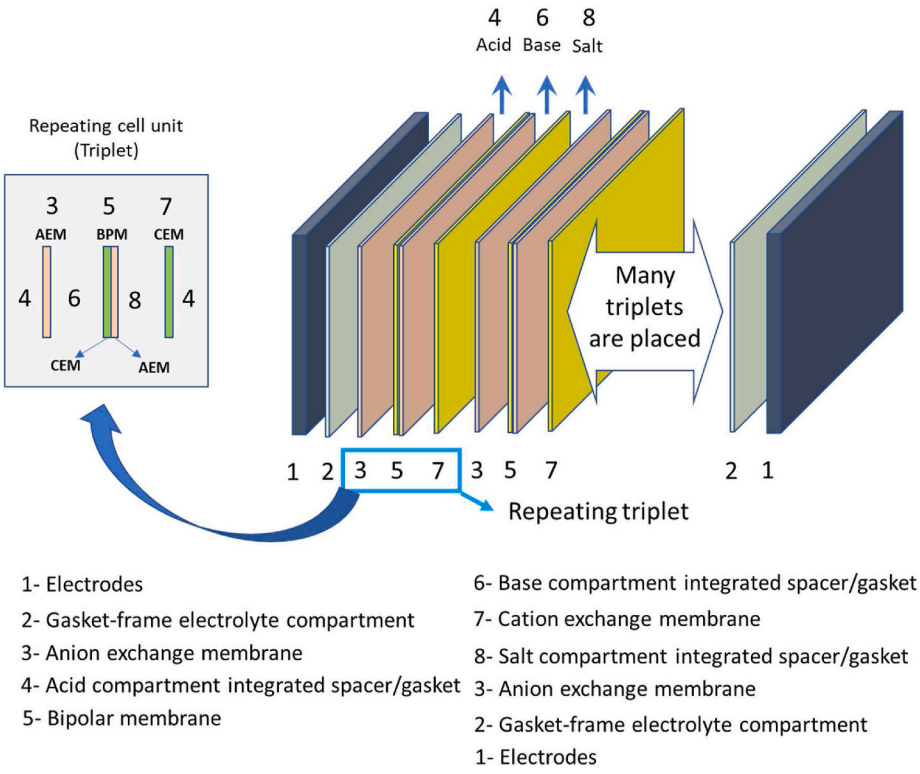

Fig. 2. Main stack and triplet components.

2.1.2. VRFB (benchmark technology)

The VRFB consists of two vanadium-based electrolytes named catholyte (V^{3+}/V^{2+}) and anolyte (V^{5+}/V^{4+}). These electrolytes are contained in separated tanks and pumped to the same stack, where a Proton Exchange Membrane (PEM) is located between them. In this way the following reaction takes place:

$$VO_2^+ + 2H^+ + V^{2+} \rightleftharpoons VO^{2+} + H_2O + V^{3+}$$

For a nominal power of 1 MW, 2 stacks with a total of 155 cells are required. Each cell comprises a PEM, a bipolar plate and two carbon felt electrodes at the sides. This assembly is tightened by a cell frame. The stack is made of a certain number of cells sealed together by a stack frame. Gaskets are used to improve the sealing. For reaching a nominal capacity of 8.3 MWh the system requires an electrolyte volume of 202 m^3. Final electrolyte concentration is 1.6 mol/l for vanadium and 2 mol/l for sulfate. Each type of electrolyte is contained in a tank that is connected to the stack by two centrifugal pumps and pipes (30 m length). Another 5 m of pipes are needed for connecting each stack. A deeper explanation of this technology can be found in the literature (Weber et al., 2018) (manuscript and supporting information files).

2.2. Environmental evaluation methodology

The LCA methodology' framework is harmonized by the ISO 14040 standard, guaranteeing the substantial consistency and quality assurance of the evaluation method, and therefore enabling further comparisons. According to the standards, the LCA studies must follow four interrelated stages: (1) goal and scope definition, (2) inventory analysis, (3) impact assessment and (4) interpretation.

2.2.1. Goal and scope definition

This section focuses on the establishment of the study scope, as well as the system boundary and the Functional Unit (FU) definition. The main objective of this analysis was to assess the environmental performance associated with the innovative AB-FB system and its comparison with the VRFB system. This approach was aimed to identify key aspects related to the production phase for improving the technology under a life cycle perspective from a cradle to grave approach.

System boundaries of the two study cases correspond to the analysis of manufacturing, operation and end-of-life (EoL) stages can be seen in Fig. 4. This means that the raw material mining, the components production processes, the assembly of each energy storage system, the use stage and the EoL stage, were considered in this analysis.

The FU is the reference to which the process inputs and outputs are correlated. It is determined by the principal function of the target products of the assessment. In this work, **1 MWh of provided or delivered electricity** was selected as FU to compare the AB-FB and VRFB technologies in a **time frame of 20 years**. The FU has been selected in agreement with the reported ones in literature. In addition, this FU is also defined by the Product Category Rules (PCR) for Electricity, steam and hot/cold water generation and distribution(EDP International AB, 2020).

2.2.2. Life cycle inventory (LCI)

The inventory analysis referred to a detailed data collection process involving all inputs and outputs (e.g., energy, materials, emissions) that can be identified within the system boundaries. This process also implied data homogenization according to the selected FU. Detailed inventory of the AB-FB and VRFB systems have been provided in the SI file related to this work. In the following sections, a general description of the main considerations regarding the LCI of the two systems is included.

It is important to highlight that LCI referred to the AB-FB manufacturing process was mostly based on foreground information provided by the BAoBaB project partners. LCI was also complemented with background information obtained from literature and particularly from the VRFB inventory, as it is described in further sections.

Regarding the VRFB system, the LCI of this system was mainly generated from raw data reported in literature (Weber et al., 2018).

LCI generated to both, the AB-FB and VRFB systems, was adapted to

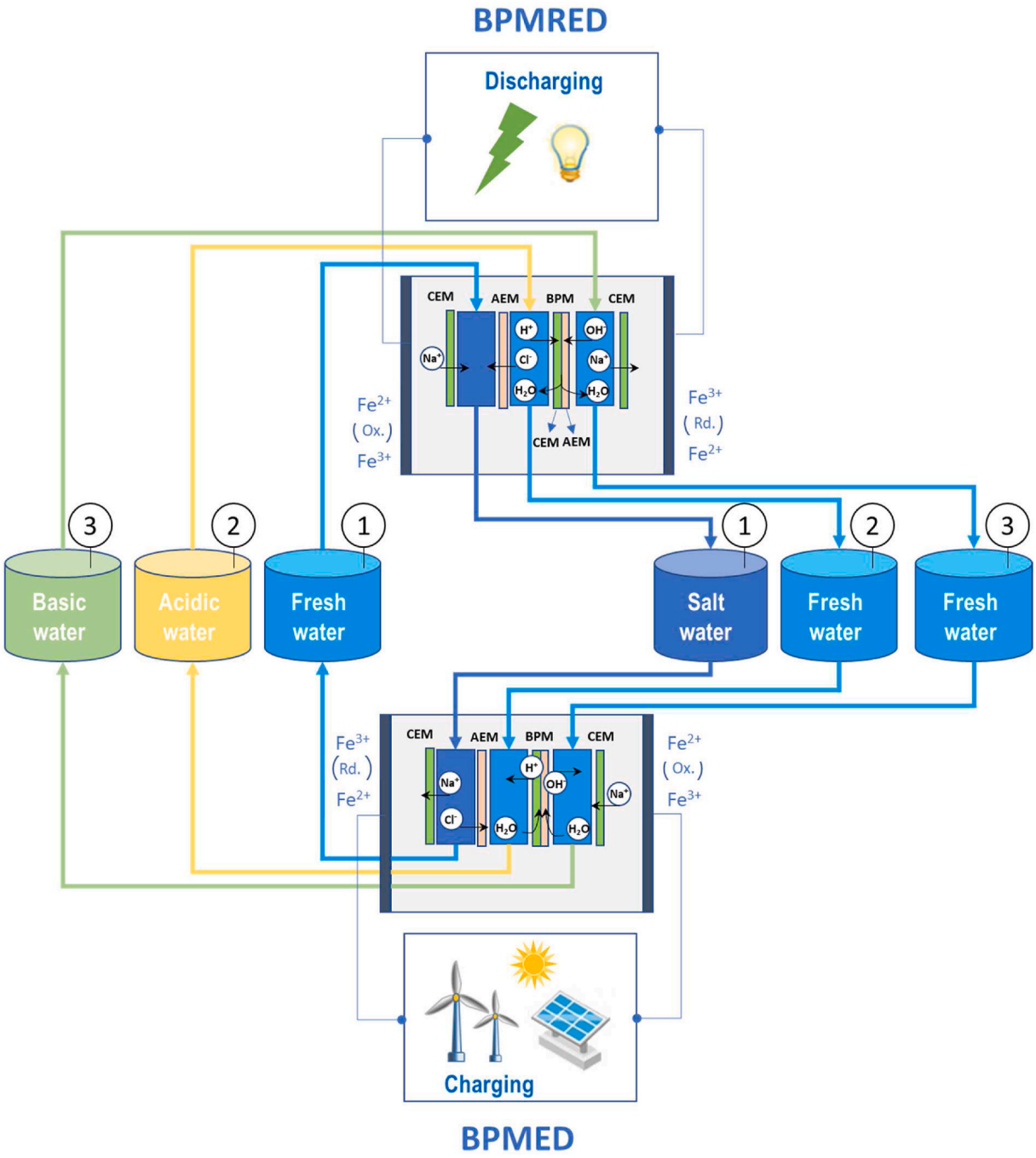

Fig. 3. Schema of reactions taking place in one single triplet-cell during the charging and discharging process of the AB-FB system. Adapted from (Culcasi et al., 2020; Pärnamäe et al., 2020; van Egmond et al., 2018).

inputs and outputs from the Ecoinvent 3.4 to be further assessed according to methodology described in section 2.2.3.

2.2.2.1. Manufacturing stage. The main battery components of the AB-FB and the VRFB systems is presented in Table 2 and Table 3. This table summarises raw and normalized datasets.

The normalized data corresponded to the amount of battery components as per FU, i.e., 1 MWh of provided electricity. To this purpose, it was primarily assumed that the service provided by the batteries came from RS for Wind or PV installations as the future application, i.e., balancing demand from the grid and daily electricity generation. This application required an average of 1.12 cycles per day, according to technical parameters found in literature (Baumann et al., 2017). Consequently, by considering a net storage capacity of 6 MWh (see Table 1), a total amount of 49056 MWh can be provided over 20 years of lifetime (see section 2.2.1), according to equation (2):

$$49056\ MWh\ provided = 1.12\frac{cycles}{day} \times 20\ years \times 365\frac{days}{year} \times 6\frac{MWh}{cycle} \quad (2)$$

It also indicated that there is a total of 8176 charge-discharge cycles. The normalization of all the inputs and outputs related to the manufacturing inventory of both systems (VRFB and AB-FB) was consequently carried out by applying equation (3):

$$normalised\ data\left(\frac{g}{MWh\ provided}\right) = \frac{raw\ data\ (g)}{49056\ MWh\ provided} \quad (3)$$

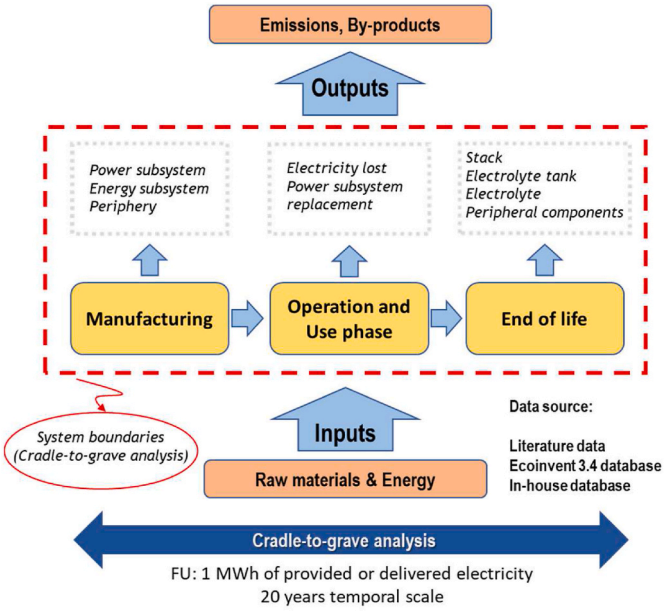

Fig. 4. System boundaries defined for the LCA.

Normalized data is expressed as g/MWh provided except for the inverter required to both systems. In this case, it is also included the amount of required inverter assembly process (p). The p unit is defined by the Ecoinvent 3.4 database used to the LCA modelling.

According to data included in Table 2, the AB-FB electrolyte weight composition was estimated as 94.42% water, 5.52% NaCl, 0.03% $FeCl_2$ and 0.03% $FeCl_3$. For the VRFB system, electrolyte weight composition was estimated as 21.2% of vanadium pentoxide, 14.5% of sulfuric acid, 0.4% of phosphoric acid and 63.9% of water, based on the LCI provided to the VRFB system (Weber et al., 2018).

Detailed information about materials used to model the LCI based on the available Ecoinvent database can be found in the SI file of this work. Virgin materials have been used to model the battery manufacturing component due to processes and possibilities of a recycling option have not been completely established yet for such type of battery systems.

Inputs concerning transportation have been based on estimations reported to the VRFB (Weber et al., 2018) (manuscript and supporting information files) and also according to existing data from Ecoinvent database. As an approximation, standard distances for chemical products, plastic, steel, and copper were used according to the Ecoinvent guidelines. Particularly, the membranes and electrodes were assumed to be produced on-site and thus, they did not require transport.

2.2.2.2. Operation stage. The LCI related to the operation stage included: i) data to quantify impacts attributed to internal losses and ii) inputs and outputs referred to maintenance activities and/or replacement of battery components. The impacts associated with the electricity provided (discharged) by the batteries to the end-user are not considered in this analysis. To quantify related impacts, it was assumed that i) internal losses were dependent on specific charge−discharge efficiency of the battery and ii) the replacement of battery power subsystem is carried out after 10 years of operation, as it is indicated in Table 1. A summary of inputs needed during battery operation is presented in Table 4 and

Table 2
LCI of the AB-FB manufacturing.

Battery components		Raw data				Normalized data (w/o catalyst)
Function	Component	Amount	Unit	Material	Weight, kg	g/MWh provided
Power subsystem	**Membranes**				**1742**	**35.5**
	CEM	7981	m^2	(s)PEEK	435	8.9
	AEM	7981	m^2	(qa)PEEK	435	8.9
	BPM					
	CE layer	7981	m^2	(s)PEEK	435	8.9
	AE layer	7981	m^2	(qa)PEEK	435	8.9
	Catalyst	7981	m^2	P4VP	2	0
	Gaskets and plates				**5331**	**108.7**
	Spacers	21831	m^2	LDPE	1949	39.7
	Gaskets	2112	m^2	LDPE	943	19.2
	Dividers	50	m^2	LDPE	851	17.3
	Endplates	65	m^2	LDPE	1588	32.4
	Electrodes				**1472**	**30.0**
	Carbon felt	65	m^2	PAN Carbon felt	17	0.3
	Current collector	65	m^2	Copper	1455	29.7
	Stack frame				**6607**	**134.7**
	Steel plates	78	m^2	Steel	6310	128.6
	Rods, bolts	0.050	m^2	Steel	297	6.1
Total power subsystem					**15153**	**308.8**
Energy subsystem	**Electrolytes**				**1955346**	**39859.5**
	Water	1846	m^3	Demiwater	1846154	37633.6
	NaCl	1846	kmol	NaCl	108,000	2201.6
	$FeCl_2$	4	kmol	$FeCl_2$	523	10.7
	$FeCl_3$	4	kmol	$FeCl_3$	69	13.6
	Reservoirs				**6145**	**125.3**
	Bags	2769	m^3	PVC	6114	124.6
	Tank	8	m^3	LDPE	31	0.6
Total energy subsystem					**1961491**	**39984.7**
Periphery	Pumps	7	units	plastic, steel	1050	21.4
	Pipes	150	m	LDPE	682	13.9
	Inverter	1	unit	Various	3000	61.2 (2.04E-5 p)
	Cables	50	m	Copper, PVC	316	6.4
	PCS	1	unit	Various	13	0.3
Total peripheral components					**5061**	**103.2**
Total					**1981705**	**40396.8**

Table 3
LCI of the VRFB manufacturing. AAdapted from (Weber et al., 2018).

Battery Components		Raw data				Normalized data
Function	Component	Amount	Unit	Material	Weight, kg	g/MWh provided
Power Subsystem	Membrane	155	Items	Nafion	150	3.06
	Electrodes					48.70
	PAN Carbon felt	310	Items	Graphite	419	8.54
	Current collector	4	Items	Copper	1970	40.16
	Bipolar plate	157	Items	PPG86 composite	5490	111.91
	Cell frame	155	Items	PVC	306	6.24
	Gaskets	310	Items	FKM	428	8.72
	Stack frame	2	Items	Steel	1253	25.54
Total power subsystem					**10016**	**204.17**
Energy Subsystem	Electrolyte	202	m^3	V_2O_5 and sulfate solution	272220	5549.17
	Tank	300	m^3	Glass fibre	32589	664.32
Total energy subsystem					**304809**	**6213.5**
Periphery	Pumps	4	Items	Plastic coated steel	580	11.82
	Pipes	70	m	Steel, Teflon lining	332	6.77
	Inverter	1	Item	Various	3000	61.15 (2.04E-5p)
	Cables	28	m	Copper, PVC	177	3.61
	PCS	1	Item	Various	13	0.27
	Heat exchanger	1	Item	Stainless steel	1023	20.85
Total peripheral components					**5125**	**104.47**
Total					**319950**	**6522**

Table 4
LCI of the AB-FB operation considering RS.

AB-FB operation		Ecoinvent 3.4	Amount	Unit
Inputs	Electricity lost	Electricity, high voltage {DE}| electricity production, wind, >3 MW turbine, onshore | APOS, U	0.54	MWh
	Power subsystem replacement		0.31	kg
Outputs		RS-wind/PV	**1.00**	**MWh provided**

Table 5
LCI of the VRFB operation considering RS (Adapted from (Weber et al., 2018)).

VRFB operation		Ecoinvent 3.4	Amount	Unit
Inputs	Electricity lost	Electricity, high voltage {DE}| electricity production, wind, >3 MW turbine, onshore | APOS, U	0.33	MWh
	Power subsystem replacement		0.20	kg
Outputs		RS-wind/PV	**1.00**	**MWh provided**

Table 5 for the AB-FB system and the VRFB system, respectively. Inputs were also referred to the FU, i.e., 1 MWh of provided electricity (output).

As it is depicted in Table 4, 0.54 MWh are lost per MWh provided due to internal inefficiencies of the AB-FB system by considering an efficiency of 65%. For the VRFB system, which is charaterized with an efficiency of 75%, 0.33 MWh are lost per MWh provided (see Table 5).

Impacts related to the electricity losses are dependent on electricity generation conditions, such as location and type of the energy sources. For the AB-FB and VRFB comparison, Germany was the selected location due to the VRFB system was assumed to be installed in this country (Weber et al., 2018). In terms of energy sources, it was defined Wind power generation because of the better performance obtained to RS for wind power installations by the VRFB system (Weber et al., 2018) compared with PV installation.

The selected energy source was modelled as Electricity, high voltage {DE}| electricity production, wind, >3 MW turbine, onshore | APOS, U, based on Ecoinvent 3.4 datasets. According to Amelang and Wehrmann (2020), turbines with a power capacity of over 3.3 MW are the dominant one in Germany.

Other scenarios in terms of location and energy source were evaluated as part of the sensitivity analysis to quantify impacts attributed to internal losses (see section 2.2.4).

2.2.2.3. End-of-life (EoL) stage. Some battery components were considered to model the EoL scenarios. The amount of each component is indicated in Table 6. They were estimated according to the LCI normalized values data depicted in Tables 2 and 3, in terms of the FU, i.e., 1 MWh of provided electricity (output). Due to the battery power subsystem replacement is carried out after 10 years of operation, 2 stacks were assumed to be required to attain the expected battery lifetime of both technologies.

The treatment of the battery components was based on a conservative scenario. The AB-FB system is still in an early stage of development and only very limited EoL data could be clearly identified at this time. For this reason, the EoL model of the AB-FB system has been carried out by applying same approaches than the ones previously defined to the VRFB system (Weber et al., 2018). Based on this study, valorisation routes such as recycling or incineration were defined to the VRFB components (stack, electrolyte tank, electrolyte and peripheral components). Same scenarios were applied to the AB-FB system components: stack (see Table 7), electrolyte tank (see Table 8), electrolyte (see Table 9) and peripheral components (see Table 10). Consequently, both technologies were assessed by the same scenarios.

The simplified approach applied to the EoL stage of the

Table 6
Amount of battery components applied to each EoL scenario.

Scenario	AB-FB	VRFB
	g/MWh	g/MWh
Stack recycling	618	408
Electrolyte tank recycling	125.3	664.3
Electrolyte recycling	39859.5	5549.2
Peripheral components	103.2	104.5

Table 7
LCI for stack recycling. Adapted from (Weber et al., 2018).

Battery stack recycling		Ecoinvent 3.4	Amount	Unit
Inputs	Used battery stack	Battery stack, 1 MW, to recycling	1.00	kg
	Electricity (disassembly)	Electricity, medium voltage {Europe without Switzerland} | market group for | APOS, U	0.01	kWh
	Fuel (disassembly)	Diesel, burned in building machine {GLO}| market for | APOS, U	0.1	MJ
Outputs	Plastic to incineration	Waste polyvinylchloride {Europe without Switzerland} | treatment of waste polyvinylchloride, municipal incineration | APOS, U	8.38E-02	kg
	Carbon felt/ BPP	Waste plastic, mixture {Europe without Switzerland} | treatment of waste plastic, mixture, municipal incineration | APOS, U	0.56	kg
	Steel, to recycler	Iron scrap, unsorted, to recycling	0.13	kg
	Copper, to recycler	Copper scrap, sorted, pressed {RER}| treatment of copper scrap by electrolytic refining | APOS, U_ (*modified without recuperation*)	0.20	kg
	Waste, to incineration	Municipal solid waste {RoW}| treatment of, incineration | APOS, U	3.39E-02	kg

Table 8
LCI for electrolyte tank recycling. Adapted from (Weber et al., 2018).

Battery electrolyte tank recycling		Ecoinvent 3.4	Amount	Unit
Inputs	Used electrolyte tanks	Electrolyte tanks, to recycling	1.00	kg
	Electricity (disassembly)	Electricity, medium voltage {Europe without Switzerland} | market group for | APOS, U	0.01	kWh
	Transport, road	Transport, freight, lorry 16–32 metric ton, EURO5 {GLO}| market for | APOS, U	0.05	t × km
Outputs	Plastic to incineration	Waste plastic, mixture {Europe without Switzerland} | treatment of waste plastic, mixture, municipal incineration | APOS, U	1	kg

Table 9
LCI for electrolyte recycling. Adapted from (Weber et al., 2018).

Battery electrolyte recycling		Ecoinvent 3.4	Amount	Unit
Inputs	Used electrolyte	Used electrolyte, to recycling	1.00	kg
	Electricity (reprocessing and purification)	Electricity, medium voltage {Europe without Switzerland} | market group for | APOS, U	4.45E-02	kWh
	Transport, road	Transport, freight, lorry 16–32 metric ton, EURO5 {GLO}| market for | APOS, U	0.6	t × km
Outputs	Electrolyte, recycled	No apply	0.95	kg

Table 10
LCI for the peripheral components (pumps, pipes, cables and electronics) recycling. Adapted from (Weber et al., 2018).

Battery peripheral components		Ecoinvent 3.4	Amount	Unit
Inputs	Used periphery	Periphery, to recycling	1.00	kg
	Electricity (disassembly)	Electricity, medium voltage {Europe without Switzerland} | market group for | APOS, U	0.01	kWh
	Fuel (disassembly)	Diesel, burned in building machine {GLO}| market for | APOS, U	0.10	MJ
Outputs	Steel, to recycler	Iron scrap, unsorted, to recycling	0.15	kg
	Copper, to recycler	Copper scrap, sorted, pressed {RER}| treatment of copper scrap by electrolytic refining | APOS, U	0.011	kg
	Cables	Used cable {GLO}| treatment of | APOS, U	0.033	kg
	Electronic waste	Waste electric and electronic equipment {GLO}| treatment of, shredding | APOS, U	0.59	kg
	Waste, to incineration	Waste plastic, mixture {Europe without Switzerland} | treatment of waste plastic, mixture, municipal incineration | APOS, U	0.22	kg

aforementioned battery components implied the following considerations:

- Recycling processes defined to steel and copper included the amount of material recovered from the process as well as the consumption of energy and materials during the waste processing.
- A recycling efficiency for copper was estimated to be 100%. Accordingly, copper recovered from used cables corresponded to 0.033 kg copper/kg peripheral components (see Table 10).
- For steel recycling, an electricity consumption around 1.8 GJ/t was defined to be required for remelting and refining steel scrap (Norgate, 2013). Recycling efficiency for steel was estimated to be 100%.
- The energy input required for battery disassembly was approximated to the one defined by the Ecoinvent process iron scrap sorting and pressing (Weber et al., 2018).
- It was assumed to both battery systems that electrolyte required some re-processing and purification at the end of expected battery lifetime (i.e., 20 years of operation), which demanded electricity consumption, according to estimations based on literature (Weber et al., 2018).
- Materials recovered by recycling of battery components, for instance, copper or steel (defined as outputs in Tables 7 and 10), were not defined as input to the battery manufacturing stage, i.e., a closed-loop recycling was not applied in this investigation. It was considered because of possibilities to apply a closed-loop recycling approach are not completely defined to this type of batteries at present.

2.2.3. Impact assessment

The environmental analysis of the AB-FB and the VRFB technologies was developed by using SimaPro software version Analyst 9.1.0.8, and in-house databases complemented by Ecoinvent 3.4. In this study, the ReCiPe 2016 v1.1 midpoint environmental method was applied, and hierarchical evaluation was conducted. The ReCiPe midpoint method is the one of the most recent and comprehensive methods currently available in life cycle impact assessment (Opatokun et al., 2017) and expresses the relative severity on an environmental impact category. This approach covers all possible environmental interventions, which defines the environmental mechanism throughout the quantification of

the impacts at intermittent stages of the cause–effect chain (Bare and Gloria, 2006).

ReCiPe involves eighteen midpoint impact categories. Among them, some indicators typically exhibit high relative impacts, according to the LCA conducted to battery technologies (Díaz-Ramírez et al., 2020a; Mcmanus, 2012; Troy et al., 2016). These indicators are presented in Table 11. They have been selected to be analysed in detail in this work because of their relevance to the aim of this study.

2.2.4. Interpretation

This stage of the LCA methodology refers to the understanding of the inventory phase results and the consequential impacts as well as the eventual draw of conclusions and recommendations for design improvement.

In this work, as part of the interpretation stage, a sensitivity analysis was carried out to assess the effect of electricity losses during the AB-FB operation stage (see inputs in Table 4). It was useful to elucidate potential routes to attain a more sustainable application of the innovative battery system.

In total, six potential applicability scenarios of the new technology were assessed by considering: i) three different energy sources for electricity generation and ii) two locations to assess the impacts due to origin of electricity generation.

Energy sources considered were:

i) wind power,
ii) photovoltaic energy, and
iii) electricity mix.

Regarding the origin of electricity production, one location was Germany (DE), representing Western Europe, due to the benchmark technology (VRFB) was assumed to be installed there (Weber et al., 2018). Another location was Italy (IT), representing Southern Europe, because this site corresponded to the place selected within the BAoBaB project for the installation of the new technology pilot scale device.

Considering Ecoinvent 3.4 datasets, electricity lost based on PV installations was modelled as *"Electricity, low voltage {IT or DE}| electricity production, photovoltaic, 570 kWp open ground installation, multi-Si | APOS, U"*.

The wind power characteristics were dependent on the location. In Germany, it is dominated by onshore turbines with a power capacity >3 MW, see section 2.2.2.2. It was modelled as *"Electricity, high voltage {DE}| electricity production, wind, > 3 MW turbine, onshore | APOS, U"*.

Installed wind power capacity in Italy is predominantly onshore with an average power capacity of 1.4 MW (IEA Wind, 2017). Then, for the Italian case, electricity lost was modelled as *"Electricity, high voltage {IT}| electricity production, wind, 1-3 MW turbine, onshore | APOS, U"*.

Finally, the electricity mix was modelled as *"Electricity, high voltage {IT or DE}| market for | APOS, U"*.

Table 11
Environmental impact indicators selected for this study with acronyms and respective units.

Environmental indicator (EI)	Acronym	Unit
Global Warming	GWP	kg CO_2 eq
Terrestrial acidification	TAP	kg SO_2 eq
Terrestrial ecotoxicity	TETP	kg 1,4-DCB
Freshwater ecotoxicity	FETP	kg 1,4-DCB
Marine ecotoxicity	METP	kg 1,4-DCB
Human carcinogenic toxicity	HTPc	kg 1,4-DCB
Human non-carcinogenic toxicity	HTPnc	kg 1,4-DCB
Mineral resource scarcity	SOP	kg Cu eq
Fossil resource scarcity	FFP	kg oil eq
Water consumption	WCP	m^3

2.3. Economic evaluation methodology

Total Capital Cost (TCC), also known as CAPEX (Capital Expenditure), and Life Cycle Costing (LCC) were the approaches considered for evaluating the costs of both ESS: AB-FB and VRFB. The selection of these methodologies was based on previous studies reported in literature (Zakeri and Syri, 2015).

Economic inputs related to the innovative AB-FB system was provided by the BAoBaB project partners according to the development path envisioned for 2025, as mentioned in section 2.2.2. Most of the costs regarding the VRFB system have been extracted from literature (Noack et al., 2016). In the case of components shared by both ESS, the same costs were applied. More detailed data regarding all the costs considered in this study were provided in the SI file related to this work.

2.3.1. TCC

TCC is the capital expenditure that must be initially done for acquiring an ESS. It evaluates the cost of each component that comprised the ESS. Particularly, it was considered the evaluation of costs related to both the Power Conversion System (PCS) and energy storage for the two studied batteries.

PCS costs are the costs of the stack or power subsystem components (including labour cost for the stack assembly) together with the periphery system and the labour related costs for the battery assembly. It is important to remark that the labour cost for the stack assembly was generated to both technologies by performing an iterative process and fixed to a monetary contribution of 5% the final stack cost, following criteria found in literature (Noack et al., 2016). In the same way, the labour related costs (also named as system assembly cost) were generated. In this case, they were assumed to represent a monetary contribution of 7% the final TCC value. Assumptions related to the labour cost for the stack and the battery assembly were made according to literature (Noack et al., 2016), and applied to both battery systems due to the lack of information from the battery manufacturer, and as a strategy to obtain a comparable result. The related cost to stack and system assembly can be found in the SI of this work.

The energy storage related costs refer to the cost of the reservoirs or tanks and electrolyte (energy subsystem components). Besides, Balance of Plant (BOP) costs are also included in the TCC. BOP costs are related to project engineering and facilities adaptation (including grid related actions) (Zakeri and Syri, 2015). In this vein, the TCC can be summarized by the following simplified formula (Noack et al., 2016; Zakeri and Syri, 2015):

$$TCC = C_{PCS} + C_{energy\ storage} \times h + C_{BOP} \quad (4)$$

Calculation of C_{PCS} corresponds to the sum of the power subsystem components' costs, as it has been mentioned previously. In the case of the $C_{energy\ storage}$, the sum of the components' costs must be multiplied by the discharge time of the battery (named here as h), which is included in Table 1 for both technologies. Data used for the calculations can be found in the SI of this work. Finally, it has been also quantified the total investment cost. It was generated as the sum of costs related to PCS and energy storage related costs.

2.3.2. LCC

The LCC is a complementary analysis to be carried out after the TCC evaluation. In this manner, the LCC analysis covered all the costs incurred by the extended waste management system (Barringer and Barringer, 2003). This approach is required in Europe for SPP (Sustainable Public Procurement), as specified in 2014/24/EU Art. 68.

This type of analysis comprised two steps: firstly, the total costs over the lifetime of the plant were calculated; secondly, these values were annualized. Concerning the first step, the LCC explores the costs over the total lifetime of the ESS in terms of initial investment (TCC), Operation & Maintenance (O&M), Replacement (R), Disposal and Recycling (DR)

Table 12
Formulae used in the LCC study. (i) Interest rate of the ESS. (T) Lifetime of the plant. (n) Number of cycles per year. (h) Discharge time. (t) Replacement time. (ηsys) system efficiency.

Parameter	Acronym	Unit	Formula	N°
Capital Recovery Factor	CRF	–	$CRF = \frac{i(1+i)^T}{(1+i)^T - 1}$	(5)
Annualized TCC	$C_{cap,a}$	€/kW-year	$C_{cap,\,a} = TCC \times CRF$	(6)
Annualized O&M costs	$C_{O\&M,a}$	€/kW-year	$C_{O\&M,\,a} = C_{FOM,\,a} + C_{VOM} \times n \times h$	(7)
Annualized future cost of replacement	$C_{R,a}$	€/kW-year	$C_{R,\,a} = CRF \times \sum_{k=1}^{r} (1+i)^{-kt} \times \frac{C_R \times h}{\eta_{sys}}$	(8)
Annualized disposal and recycling cost	$C_{DR,a}$	€/kW-year	$C_{DR,\,a} = C_{DR} \times \frac{i}{(1+i)^T - 1}$	(9)
Annualized external environmental cost	$C_{EE,a}$	€/kW-year	$C_{EE,a} = C_{EE} \times \frac{i}{(1+i)^T - 1}$	(10)
External environmental cost	C_{EE}	€/kW	$C_{EE,i} = EI_i \times ECF_i$	(11)
Annualized LCC costs	$C_{LCC,a}$	€/kW-year	$C_{LCC,\,a} = C_{cap,a} + C_{O\&M,a} + C_{R,a} + C_{DR,a} + C_{EE,a}$	(12)
Levelised Cost of Electricity	LCOE	€/kWh	$LCOE = \frac{C_{LCC,\,a}}{n \times h}$	(13)
Net Levelised Cost of Storage	LCOS	€/kWh	$LCOS = LCOE - \frac{price\ of\ charging\ power}{\eta_{sys}}$	(14)

and External Environmental (EE) (Zakeri and Syri, 2015). With respect to the second step, the formulae used for annualising the total costs over the lifetime are collected in Table 12.

The main considerations related to each annualized cost are explained below:

- Capital Recovery Factor: for calculating the CRF, the annual interest rate (also known as discount rate) was taken from the literature as 7.7% (Poonpun and Jewell, 2008). The lifetimes of the plants were established as 20 years (Table 1).
- Annualized TCC ($C_{cap,a}$): corresponded to the annualized investment cost.
- Annualized O&M costs ($C_{O\&M,a}$): this cost was divided into variable and fixed O&M costs. Variable O&M cost were calculated knowing the average value of variable O&M costs from reference (Zakeri and Syri, 2015): 0.9 €/MWh. In the section related to the manufacturing stage of the ESS (2.2.2.2) was stated that the ESS performs 1.12 cycles per day, a total of 8176 charge-discharge cycles over the system lifetime of 20 years, which means the performance of 408 cycles per year. These data were needed for calculating $C_{O\&M,a}$.

The annualized variable O&M costs were based on the theoretical value 0.9 €/MWh (Zakeri and Syri, 2015) and the yearly operating hours (Table 12).

- Annualized future cost of replacement costs ($C_{R,a}$): this cost was calculated considering the replacement of the stack components as well as the stack assembly cost after 10 years of operation (i.e., replacement time). Stack composition can be seen in the LCI tables (VRFB: Table 3 and AB-FB: Table 2). System efficiency and discharge time can be found in Table 1.
- Annualized disposal and recycling costs ($C_{DR,a}$): this cost was primarily comprised by the C_{DR}. The C_{DR} was calculated according to the cost of the recycling processes considered in reference (Weber et al., 2018) for the stack, the tank, the electrolyte and the periphery system. Additional information was obtained from Table 7 to Table 10). Just the costs of electricity and fuel were contemplated for the different processes. In the case of the recycling process for the electrolyte there was a difference between the AB-FB and the VRFB systems. In the case of the VRFB system, the process of electrolyte re-balancing was applied and resulted to 0.04 kWh/kg of electrolyte (Weber et al., 2018), therefore the electricity cost was higher for this system. For the AB-FB system, 0.01 kWh/kg of electrolyte was assumed, as this value was the one considered for the rest of the components (stack, tank and peripheric system). For monetizing the electricity, the price of charging power was 0.3 €/kWh (Noack et al., 2016). Fuel cost was computed considering a calorific power equal to 37.5 MJ/l, density equal to 0.85 kg/l and price of heating gas oil equal to 0.56 €/l (European Commission, 2020b). Additional data is provided in SI file related to this work.
- Annualized external environmental costs ($C_{EE,a}$): this cost was calculated following the formulae included in Table 12 being dependent on the external environmental cost.
- External environmental cost (C_{EE}): C_{EE} refers to the costs linked to the environmental impacts (EIs) obtained from the LCA. As described in section 2.2.2.2, the selected service was the RS for wind power installations located in Germany.

Among all the indicators considered to the LCA (see Table 11), toxicity and ecotoxicity categories were excluded from this study. For ecotoxicity and toxicity factors, the final values involve a great uncertainty. Particularly, criteria to exclude Terrestrial ecotoxicity, Freshwater ecotoxicity and Marine ecotoxicity were based on literature (Danny Wille, OVAM, Stationsstraat 110, 2018). Reasons to omit evaluation of Human carcinogenic toxicity and Human non-carcinogenic toxicity as part of the external environmental costs are mostly based on their dependence on the ecosystem type (De Bruyn et al., 2018). Therefore, just the following EIs were considered: **Global Warming, Terrestrial Acidification, Mineral Resource Scarcity, Fossil Resource Scarcity and Water Consumption.**

These impacts were converted to economic values using External Cost Factors (ECFs) referred to 2015 prices provided by literature and related to 2015 prices (De Bruyn et al., 2018; De Nocker and Debacker, 2018; Díaz-Ramírez et al., 2020a). For the present analysis, those values were updated to 2020 prices by applying an annual inflation rate of 3%.

The updated ECFs to 2020 prices are shown in Table 13. Additional data was included in the SI file related to this work.

The C_{EE} of each EI ($C_{EE,\,EI}$) was then calculated as the product between EI result (EI unit/kWh of provided electricity) and ECF (€/EI unit). Finally, the total C_{EE} corresponds to the sum of the single $C_{EE,\,EI}$.

- Annualized LCC costs, ($C_{LCC,a}$): this cost was calculated following the formulae included in Table 12 and corresponded to the sum of the previously described annualized costs.
- Levelized Cost of Electricity (LCOE): is a measure of the average net present cost of electricity generation for a generating plant over its lifetime. It was calculated following the formulae included in Table 12.
- Net Levelized Cost of Storage (LCOS): expresses the full capacity cost for the investor discounted over the number of discharging hours (NDH). This cost was calculated following the formulae included in Table 12.

Table 13
ECF to monetarism the EI (Adapted from Díaz-Ramírez et al., 2020a).

Environmental Indicator		Unit	(€/Unit EI)
Global Warming	GWP	kg CO_2 eq	0.063
Terrestrial acidification	TAP	kg SO_2 eq	27.208
Mineral resource scarcity	SOP	kg Cu eq	0.000
Fossil resource scarcity	FFP	kg oil eq	0.007
Water consumption	WCP	m^3	0.073

As it can be noticed, the final result of the LCC is composed of the Levelised Cost of Electricity (LCOE) and the net Levelised Cost of Storage (LCOS), according to formulae in Table 12. However, most of the studies reported in literature have generally indicated ESS costs based on the TCC (Chen et al.,; Ferreira et al., 2013; Ibrahim et al., 2008) because of the lack of data regarding the long-term utilization of the ESS.

3. Results and discussion

3.1. Environmental implications

3.1.1. General overview of AB-FB and VRFB manufacturing

According to the LCI normalized data (see Table 2 and 3), the weight percentage distribution among the three subsystems is similar between the AB-FB and the VRFB technologies (see Fig. 5), with the energy subsystem being by far the dominating one in terms of mass share. In this subsystem, the electrolyte is the major component and, far behind, the storage equipment. This tendency is typically the one expected to such type of batteries, as it has been reported in literature (Fernandez--Marchante et al., 2020; Gouveia et al., 2020a; Morales-Mora et al., 2021). Particularly, the AB-FB the electrolyte, which is mostly constituted by water, represents 98.7% of the total system composition (see Fig. 5), whereas the remaining components together account only for almost 1.5% of the battery composition. This is all due to the relatively low energy density of the AB-FB system. By considering the LCI normalized data of the two technologies, the total weight of the AB-FB system is 40.40 kg/MWh provided compared to 6.52 kg/MWh provided for the VRFB system.

Despite similarities identified in terms of the battery composition, significant differences were elucidated regarding the environmental burden of both systems. Fig. 6 depicted the main results obtained to the battery subsystems for both technologies (AB-FB and VRFB) represented as percentage normalized to the maximum value in each indicator.

Concerning the AB-FB system, the power components exhibited the more relevant contribution in almost all the assessed impact categories included in Fig. 6, followed by the peripheral components. One exception was the WCP indicator. In this case, the dominant contributor to the environmental impact was the energy subsystem. It can be explained by the battery composition. As it was mentioned, the electrolyte is mostly constituted by water, representing almost 99% of the total battery weight, and therefore it is mainly responsible of the impact attained in this category. Nevertheless, as depicted in Fig. 6, the AB-FB water-based electrolyte environmental related impacts did not contribute significantly to most of the analysed categories, which is an important advantage of the innovative system compared to the VRFB system. This result indicated that the electrolyte has a significant influence on the global environmental performance of the manufacturing stage of this type of batteries, in agreement with literature (Gouveia et al., 2020b).

Results for the three VRFB subsystems exhibited a similar trend to the one defined by the weight distribution. According to Fig. 6, the battery components associated with the energy subsystem (i.e., electrolyte and storage equipment) were responsible for the total impact attained to all the assessed indicators. This fact is explained by the contribution of inputs and outputs involved to produce the vanadium-

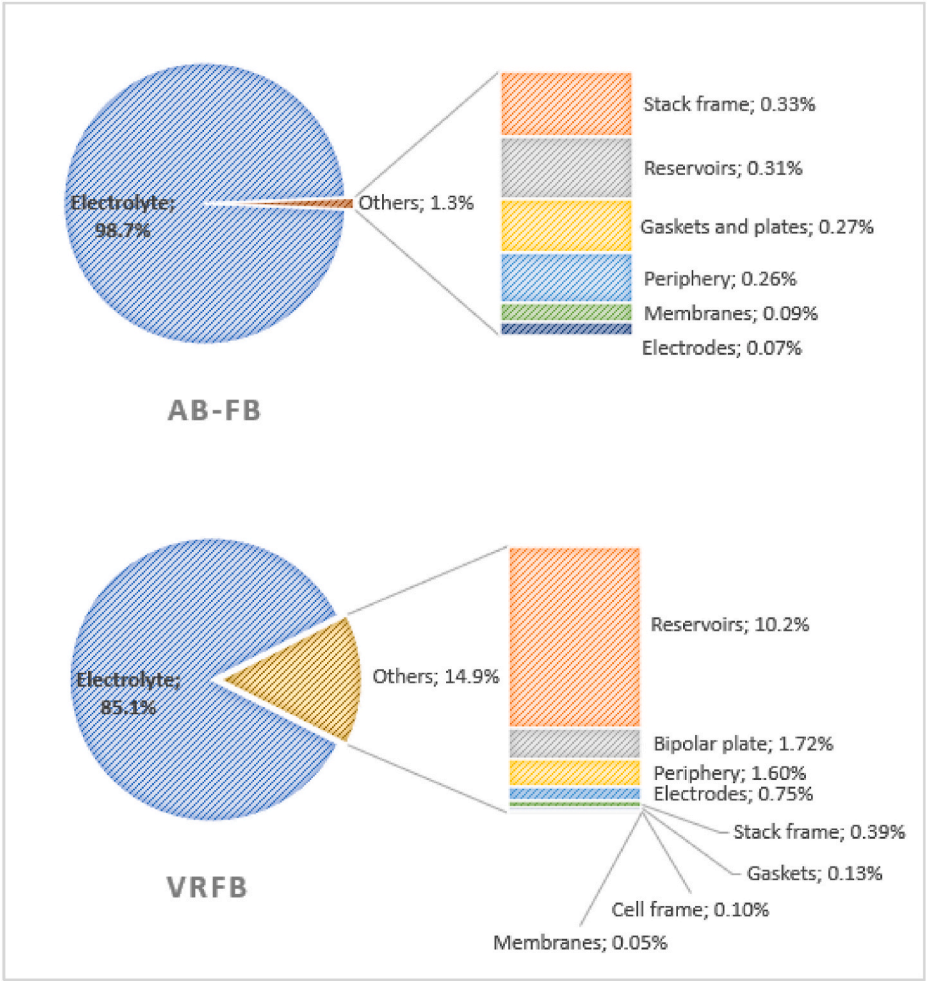

Fig. 5. Weight percentage distribution of battery components.

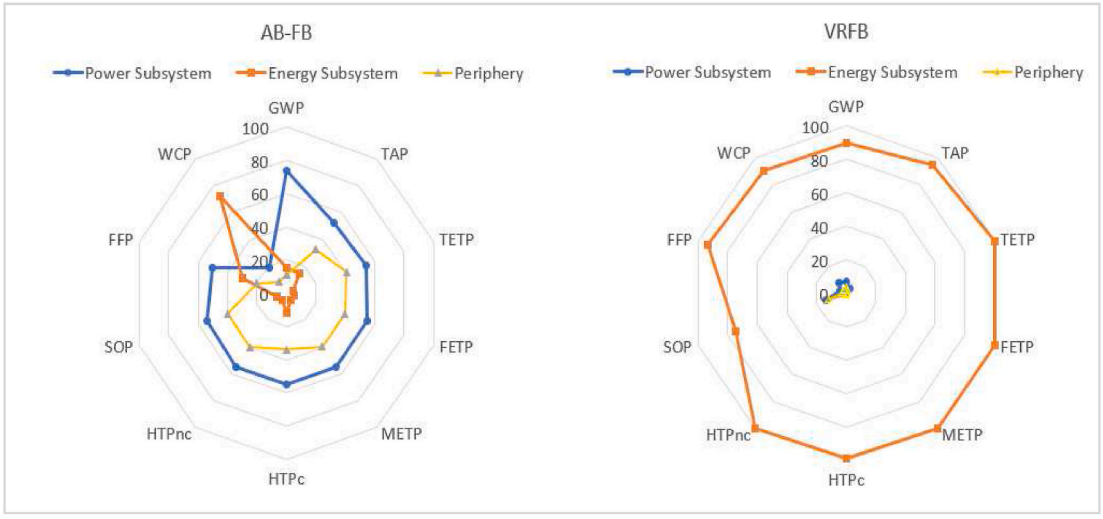

Fig. 6. LCA Normalized percentage results in terms of the battery subsystems.

based electrolyte. Upstream processes related to the electrolyte production not only comprise raw material extraction (mining) but also it is required transoceanic transport of the electrolyte from South Africa to Europe, which results into a significant environmental burden. All of the other VRFB system components exhibited only minor contributions to the environmental impact quantified to all the assessed indicators. This tendency has been also reported to other VRFB system configurations (Gouveia et al., 2020a).

These results have remarked the relevance that the electrolytes have in terms of the environmental performance of the manufacturing stage of this type of batteries and also highlight needs to develop VRFB systems with better electrolyte performance.

3.1.2. *Assessment of the AB-FB subsystem and components*

A deeper analysis of the environmental impact related to the three AB-FB subsystems was carried out to identify the most relevant drivers related to each indicator. Firstly, a general picture was obtained by the comparison of results attained to all the components, as depicted in Table 14.

According to these results, the electrodes generally composed the main contribution to the overall impact in six of the selected indicators. Membranes were the component mostly affecting GWP. The stack frame attained the more significant environmental burden in the HTPc indicator. Gaskets were generally responsible for impacts in the FFP indicator. Finally, electrolyte was the key component concerning the WCP impact category.

Secondly, the LCA Normalized percentage results were represented separately per components corresponding to each battery subsystem, as it is shown in Fig. 7. In terms of the power subsystem, it is evident the relevant influence of electrodes in most of the assessed indicators (see Fig. 7-a). Regarding the energy subsystem (see Fig. 7-b), the electrolyte was the main contributor in all the indicators, as it was expected due to reasons indicated previously by the battery composition. For the peripheral components (see Fig. 7-c), the inverter can be denoted as the main responsible for the environmental burden attributed to this subsystem in all the assessed indicators.

Per each subsystem, a network analysis with a node cut-off of 5%, (i.e., evaluation of flows with contribution higher than 5% of the total impact in the assessed indicator) was done to elucidate contribution to the assessed impact indicators in terms of materials that constituted the

Table 14
Absolute values attained for the EI in terms of the AB-FB components.

EI	Unit	Total impact	Power subsystem				Energy subsystem		Peripheral components				
			Membranes	Gaskets and plates	Electrodes	Stack frame	Electrolyte	Reservoirs	Pump	Pipes	Inverter	Cables	PCS
GWP	kg CO_2 eq	7.52	4.29	0.41	0.29	0.57	0.73	0.41	0.09	0.04	0.63	0.06	3.8E-03
TAP	kg SO_2 eq	0.03	2.2E-03	1.3E-03	0.01	2E-03	3.4E-03	1.0E-03	9.8E-04	1.2E-04	6.5E-03	2.1E-03	1.9E-05
TETP	kg 1,4-DCB	125	1.64	0.25	63.93	2.37	5.42	0.40	5.29	0.02	32.67	12.95	0.05
FETP	kg 1,4-DCB	0.97	0.01	3.8E-03	0.46	0.05	0.05	4.3E-03	0.04	2.4E-04	0.26	0.09	1.3E-03
METP	kg 1,4-DCB	1.4	0.02	5.3E-03	0.67	0.07	0.07	6.0E-03	0.05	3.4E-04	0.37	0.14	1.9E-03
HTPc	kg 1,4-DCB	0.70	0.02	0.01	0.11	0.24	0.05	0.03	0.04	1.2E-03	0.17	0.02	7.5E-04
HTPnc	kg 1,4-DCB	34.3	0.47	0.09	16.96	1.41	1.57	0.11	1.23	6.1E-03	8.99	3.44	0.05
SOP	kg Cu eq	0.1	1.6E-03	2.3E-04	0.04	0.02	6.0E-03	2.5E-04	7.2E-03	2.1E-05	0.02	7.4E-03	1.0E-04
FFP	kg oil eq	1.15	0.16	0.22	0.08	0.12	0.17	0.17	0.02	0.02	0.17	0.02	9.3E-04
WCP	m^3	0.11	9.0E-03	3.5E-03	4.6E-03	3.7E-03	4.8E-02	3.2E-02	7.6E-04	4.0E-04	7.3E-03	1.0E-03	3.1E-05

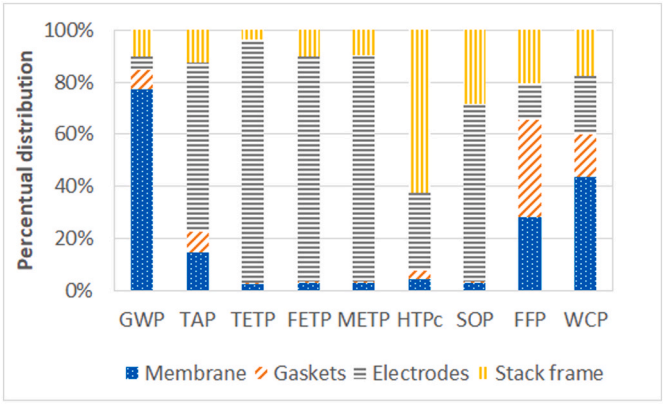

a) Power subsystem

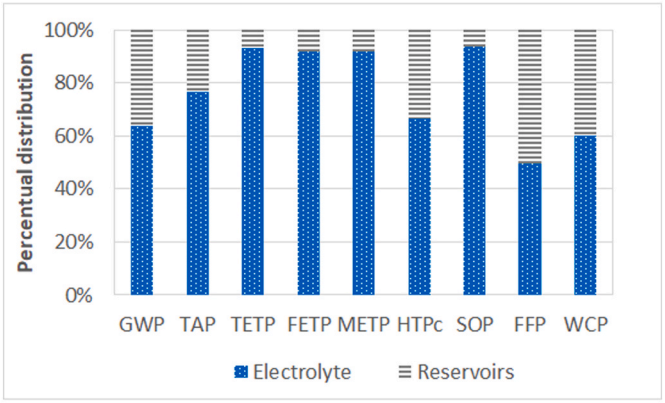

b) Energy subsystem

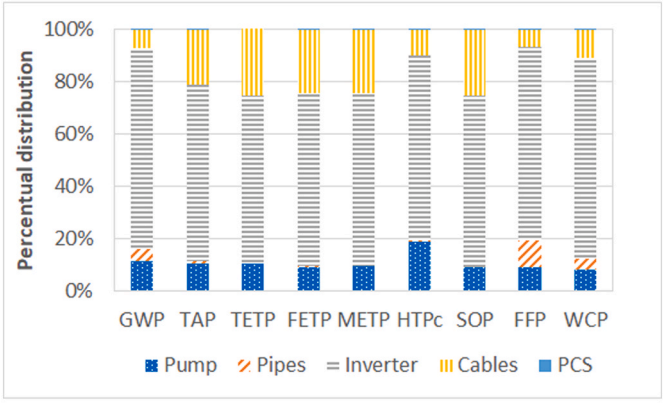

c) Peripheral components

Fig. 7. Breakdown of environmental impacts from AB-FB battery power subsystem components. LCA results are presented as Normalized percentage values.

different battery components. Results were assessed per each indicator as follows:

- Global warming potential, GWP (kg CO2 eq.):

Impacts related to the GWP were dominated by the power subsystem, as depicted in Fig. 6 and Table 14. Based on a detailed comparison of the related components in this subsystem (see Fig. 7-a), membrane manufacturing was responsible for almost 80% of the total impact attained in this indicator. Key materials concerning impacts attributed to membranes were sodium nitrate and aniline. Stack frame represented 10% of the overall power subsystem environmental impact, mostly related to the steel consumption for the stack frame manufacturing. Gaskets and electrodes had approximately a similar contribution.

- Terrestrial acidification potential, TAP (kg SO2 eq.):

Again, power subsystem depicted the more significant effect in this indicator (see Fig. 6 and Table 14) followed by the energy subsystem. Among the power subsystem components (see Fig. 7-a), the current collector in electrodes was the main responsible for the total acidification impact. This effect was related to copper production because the ore mainly consists of copper sulphide ($CuFeS_2$). Copper production is associated with emissions of sulphur dioxide (SO_2) to the air, responsible for the overall TAP impacts.

- Toxicity and ecotoxicity categories, (kg 1,4-DCB):

Based on results in Table 13, around 55% of the environmental burden was due to the power subsystem components and around 40% was mostly attributed to the peripheral components. With respect to the power subsystem, impacts were dominated by the electrodes (see Fig. 7-a).

A network analysis with a node cut-off of 5% indicated that copper production required to current collector in electrodes was responsible for the global impact of the majority ecotoxicity categories. The remaining impact was also related to copper consumption, mostly needed for the inverter and with a minor fraction required for cables manufacturing. Generally, impacts were related to the production stage from the ores.

For the HTPc indicator, it was determined by a network analysis with a node cut-off of 5% that the low-allow steel production consumed for the stack frame was the main responsible for the impact attained in the HTPc indicator together with a minor contribution of the current collector required for the electrodes. Similar tendency was obtained due to consumption of this material for the inverter and cables. The extraction of copper needed to the current collector manufacturing was the most important driver for the HTPnc indicator. The remaining impacts were mostly affected by copper required to the inverter and cables.

- Mineral resource scarcity, SOP (kg Cu-eq):

In this case, a similar tendency was observed to the one assessed for the ecotoxicity indicators (see Fig. 6 and Table 14). Impacts were mostly related to the copper production required by the current collector in electrodes. The second important power component contributor to the total battery impact in the SOP indicator was the stack frame (see Fig. 7-a) because of the consumption of low-allow steel needed for its manufacturing. This material was also responsible of impacts associated to the peripheral components. Again, impacts in this subsystem were mostly attributed to the inverter (see Fig. 7-c) due to copper and steel needed to its production.

- Fossil resource scarcity, FFP (kg oil eq):

In this indicator, the more relevant contribution to the environmental impact is due to the power subsystem and, specifically, to the gaskets manufacturing (see Fig. 7-a). A network analysis with a node cut-off of 5% indicated that polyethylene required to produce LDPE for the gaskets is the key material in the obtained environmental burden. The electrolyte and reservoirs in the energy subsystem and the inverter in the peripheral components had similar contribution. Sodium chloride consumption was responsible for the impact attributable to the electrolyte whereas polyvinylchloride emulsion was the key material referred to reservoirs. In terms of the peripheral components, lubricant oil used to the inverter production was identified as the primary responsible for the attained impact.

- Water consumption, WCP (m3).

The energy subsystem was the more significant contributor of the overall environmental impact in this indicator, i.e., around 70% of the total impact in this indicator (see Table 14). According to Fig. 7-b, the electrolyte production represented 60% of the total impact attributed to the energy subsystem. By the network analysis, this impact is due to consumption of demineralised water. Consumption of polyvinylchloride emulsion to the reservoirs manufacturing was responsible for the remaining impact attributable to the energy subsystem. In terms of power subsystem, results were mostly attributable to the production of sodium nitrite required to the membranes.

3.1.3. Cradle to grave comparison

The LCA results of the VRFB and the AB-FB systems from the cradle-to-grave comparison (whole life cycle from manufacturing to EoL) of the two systems were included in Table 15. This comparison is based on the scenario of renewables support (RS) for Wind power generated in Germany and represent impacts attributed to 1 MW of provided or delivered electricity, i.e., the FU. Environmental impact results attained for each battery life cycle stage are also shown in Fig. 8.

As visualised in Table 15, generally, the AB-FB system attained the lowest impact in almost all the assessed indicators. Compared to other flow battery technologies based on recent studies, (BEDFB, bipolar electrodialysis flow battery (Morales-Mora et al., 2021) and redox flow batteries based on Vanadium (VRFBs) and Zinc/Cerium (Fernandez--Marchante et al., 2020)), the innovative AB-FB system is also favourable. Particularly, in terms of manufacturing stage, it has been reported 9.1 kg CO_2/MWh provided (Morales-Mora et al., 2021) against 7.52 kg CO_2/MWh provided, which was quantified to the innovative AB-FB system.

As can be seen in Table 15, TETP, FETP, METP, HTPc, and HTPnc, EIs related to toxicity and ecotoxicity categories showed the most significant differences between the AB-FB and VRFB technologies, being the sum of all of them 1141 kg 1,4-DCB and 7.2E+16 kg 1,4-DCB, respectively. The main input for the ecotoxicity impacts came from the manufacturing stage (see Table 15) and more specifically from the energy subsystem, mostly due to the electrolyte manufacturing (see Fig. 6) and its transoceanic transport (Gouveia et al., 2020a).

Furthermore, as it can be identified by Fig. 8, comparison of the three life cycle stages of both systems elucidated that the manufacturing stage of VRFB represented more than 40% of the total impact in all the indicators and therefore, it was the less favourable one among the VRFB life cycle stages. For the AB-FB case, O&M was the stage with the main contribution to the total environmental impact generated during the entire life cycle of the AB-FB system. It represented more than 70% of the impact quantified in all the indicators (see Fig. 8).

Regarding the VRFB manufacturing stage impacts, it is important to indicate that the replacement of the Nafion membrane material in VRFB has been investigated (Weber et al., 2018). It was reported to be substituted by the sulfonated polyether ether ketone (sPEEK) membranes, which is one of the most promising alternatives to the common Nafion membrane material. Based on the comparative assessment of the two materials, it was concluded that the use of sPEEK instead of Nafion as membrane material decreased the environmental impacts in all the assessed categories. Generally, a high reduction potential (more than 20%) was attained to these categories. Tetrafluoroethylene and hexafluoroethane required for the Nafion synthesis process seems to be the main contributors to the environmental impacts related to the Nafion membrane production (Weber et al., 2018).

However, benefits of using sPEEK membrane did not substantially improve the total life cycle impact of the VRFB system compared with

Fig. 8. LCA Normalized percentage results comparison of AB-FB and VRFB based on Nafion membranes.

Table 15
Life cycle impacts for both batteries from a cradle to grave perspective.

		AB-FB				VRFB			
Environmental indicator (EI)	Unit	Total	Manufacturing	O&M	EoL	Total	Manufacturing	O&M	EoL
GWP	kg CO_2 eq	36.60	7.52	23.48	5.59	46.86	30.54	13.16	3.16
TAP	kg SO_2 eq	0.19	0.03	0.15	0.01	0.57	0.47	0.10	0.00
TETP	kg 1,4-DCB	831.14	125.00	636.58	69.55	7.22E+16	7.22E+16	437.08	27.11
FETP	kg 1,4-DCB	32.29	0.97	31.04	0.28	3.27E+11	3.27E+11	19.37	0.26
METP	kg 1,4-DCB	40.12	1.40	38.30	0.42	3.03E+13	3.03E+13	23.97	0.37
HTPc	kg 1,4-DCB	5.83	0.70	5.00	0.14	41.24	38.08	3.07	0.09
HTPnc	kg 1,4-DCB	231.14	34.33	187.79	9.02	1.85E+12	1.85E+12	127.45	7.54
SOP	kg Cu eq	1.14	0.10	0.66	0.02	1.29	0.39	0.43	0.01
FFP	kg oil eq	0.78	1.15	4.67	1.46	0.83	9.24	2.91	0.26
WCP	m^3	7.28	0.11	0.23	−0.02	12.42	0.39	0.16	0.01

the AB-FB system results. The LCA modelling of the VRFB system based on the two membranes implied only less than 3% reduction of the total battery impact in each indicator. This result is explained due to the power susbystem depicted a lower contribution than the energy subsystem to the total battery manufacturing impacts. As depicted in Fig. 6, the VRFB energy subsystem was the key one in terms of the battery manufacturing impacts.

Concerning the AB-FB system, a more detailed analysis of the O&M impact distribution is done in Fig. 9. Results suggested that main contribution is attributed to the battery service as RS, particularly, because of the electricity lost during the operation stage. To gain more insight the significant influence of the electricity lost, it was carried out a sensitivity analysis of conditions affecting this impact in section 3.1.4.

3.1.4. Assessment of AB-FB operation renewables support (RS) for wind or PV installations

As mentioned in section 2.2.4, as part of the sensitivity analysis some scenarios were compared to evaluate impacts related to operation of the AB-FB system of the case study based on Wind power generation. The effect of electricity losses was assessed by considering three different energy sources (i.e., wind power, photovoltaic energy and electricity mix) as well as two locations of energy production (i.e., Germany representing Western Europe and Italy representing Southern Europe). In Fig. 10, results attained for the selected environmental indicators were referred to the FU defined as 1 MW of provided or delivered electricity.

It can be noticed that for both locations, electricity based on the grid yielded the most significant impact in almost all the categories, as it has been also reported to another flow battery system (Morales-Mora et al., 2021). Generally, similar trends were observed for the renewables in both locations. Based on a network analysis of the results, differences regarding wind power and solar energy results referred to the same location were mostly related to materials required for the construction of each installation type.

The best performance was identified to the RS for wind installations in nearly all the indicators, which highlighted the beneficial service of the innovative AB-FB to support Wind installations. The only exception was found in some of the ecotoxicity and toxicity categories, mostly affected by the wide variety of substances necessary to produce wind turbines and PV panels, according to a network analysis of the indicators.

Based on results attained to the different energy sources and origin comparison, it can be suggested that the use of AB-FB system for renewable support is particularly beneficial for Wind power installations compared to PV energy. This case was determined to be the application with the lower environmental impact and therefore, recommended as the most sustainable one.

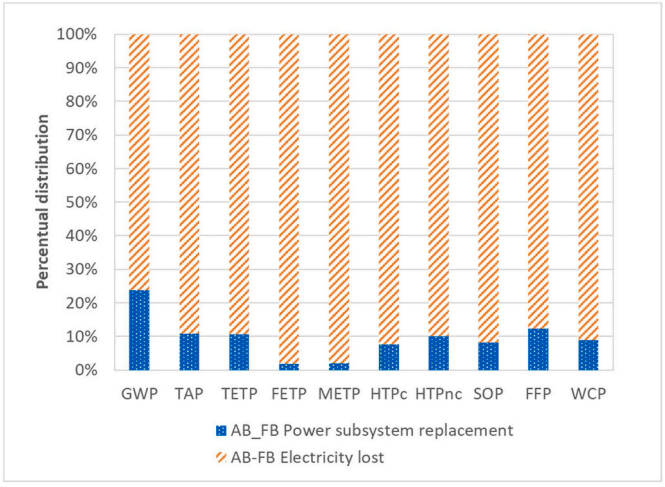

Fig. 9. LCA Normalized percentage results of the AB-FB O&M stage.

3.2. Economic results

3.2.1. TCC results

TCC values for both systems are summarised in Table 16. As mentioned in section 2.3.1, the cost of the PCS included the costs of the stack, periphery system and the labour related costs. C_{BOP} was considered the same for both systems, and the value was obtained from the literature as an approximation for VRFB (25 €/kW) (Zakeri and Syri, 2015).

As can be seen in Table 16, the most noticeable difference was related to the cost of energy storage, being the VRFB cost almost four times the AB-FB one. This difference arose from the required amount of the vanadium electrolyte and cost. Although the amount of electrolyte for the VRFB system was around 9 times lower than the corresponding one for the AB-FB system (i.e., 202 m^3 and 1846 $m^{3,}$ respectively), in terms of cost, the VRFB electrolyte was hundred times higher than the one for the AB-FB case (i.e., 5.01 €/l and 0.057 €/l, respectively). It resulted to a huge difference of almost ten times between the VRFB and the AB-FB electrolyte costs (i.e., 1012 k€ and 105 k€, respectively). Therefore, it could be said that the key cost driver for the VRFB system was the electrolyte cost. In addition, VRFB was made of more expensive gaskets, and more amount of carbon electrode material was required due to its configuration. Concerning the latter, 1 pair of carbon electrodes was needed per stack in the case of AB-FB (36 stacks), whereas for VRFB, 1 pair is needed per cell (155 cells), which resulted in a higher amount of carbon electrodes needed for VRFB system.

Capacity related costs of the assessed VRFB system were lower than some studies found in the literature. The CPS and the energy storage system costs have been estimated an equal to 289–495 €/kWh for 100 kW to 1 MW scale VRFB (Kear et al., 2012). However, it is important to highlight that this study was done in 2011 and therefore, the components costs must have been updated so far. It has been also found a revision of different VRFB costs studies (Jülch, 2016). They concluded that the capacity related cost of a VRFB system was in the range of 162–283 €/kWh, depending on the system configuration. The energy storage cost for the VRFB system analized in this work was 149 €/kWh (i.e., 1234 €/kW divided by 8.3h). Consequently, it might be said that the assessed VRFB system would be inside the range of Verena's cost estimations.

3.2.2. LCC results

Following the methodology indicated in section 2.3.2, and more specifically the formulae in Table 12, the LCC was calculated for both systems. The LCC results were included in Table 17.

In the case of O&M costs, as can be seen in Table 17, a higher cost was accounted to the AB-FB system as the discharge time of this battery was higher (9.7 h versu 8.3 h). In this way, $C_{O\&M,a}$ was a little bit higher for the AB-FB system.

For both types of ESS, $C_{R,a}$ was nearly 0, as both systems considered the same interest rate. However, the C_R was 166.5 €/kWh for the VRFB and 131.3 €/kWh for AB-FB. This result was induced by the difference in the VRFB material costs in comparison with those materials in the AB-FB system, especially the higher costs of the VRFB electrolyte, as it was previously discussed. This component resulted to be the most expensive component in the VRFB in agreement with results reported in literature to this battery type (Fernandez-Marchante et al., 2020; Rodby et al., 2020). Other cost of relevance in the VRFB system were the gaskets, as well as the ones related to the amount of carbon electrode material, as mentioned in section 3.2.1.

In the case of the EoL costs, the key cost driver was the expenditure of electricity due to rebalancing, dismantling, and recycling processes done on the electrolyte. The differences from one system to another were the larger amount of electrolyte in the AB-FB system (1846 m^3 of water vs. 202 m^3 of vanadium electrolyte), and the lack of rebalancing process for

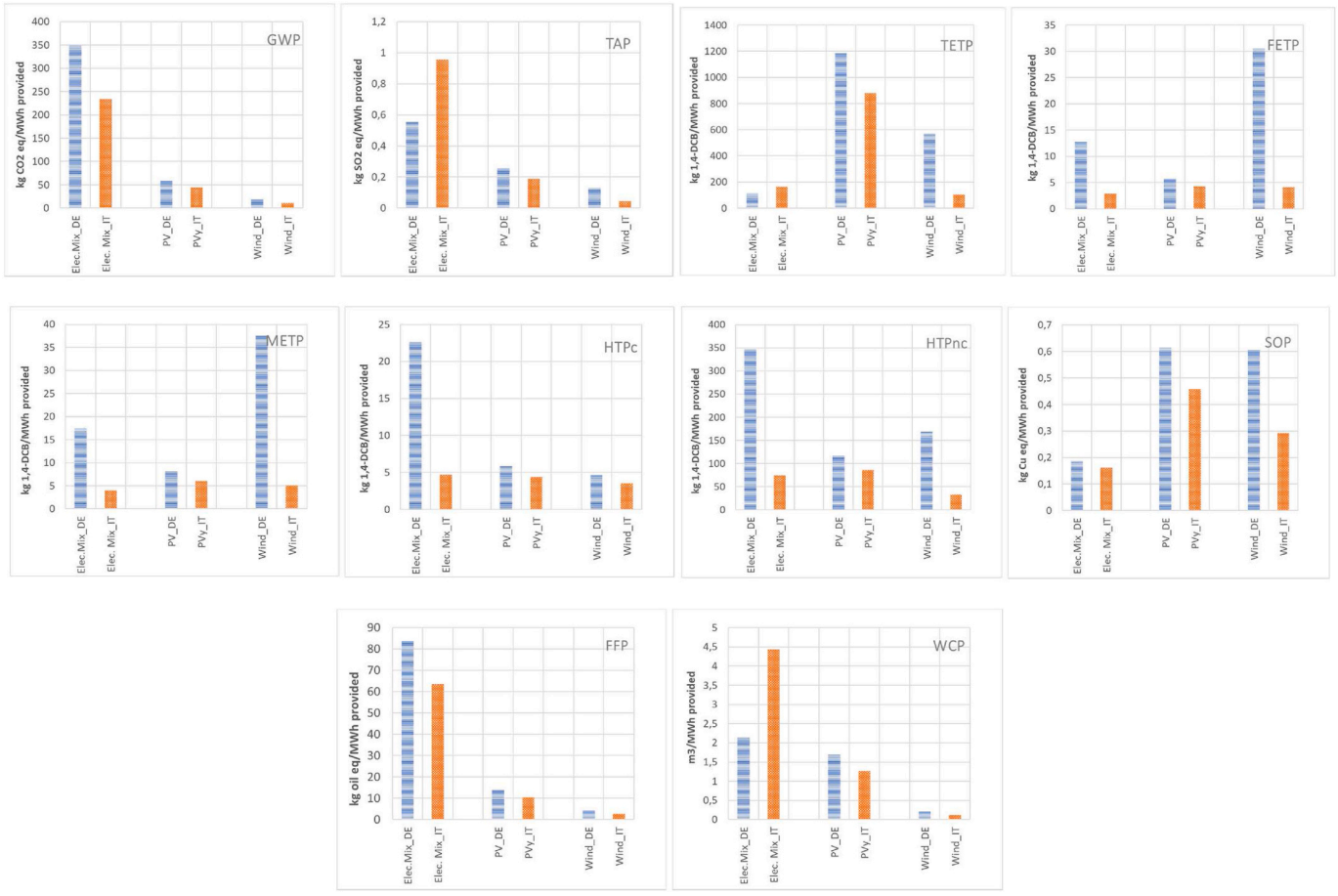

Fig. 10. Comparison of impacts related to the electricity lost attained by the AB-FB system at different operation scenarios.

Table 16
VRFB 1 MW/8.3 MWh and AB-FB 1 MW/9.7 MWh: TCC breakdown.

Parameter	Acronym	VRFB	AB-FB	Unit
Cost of power conversion system	C_{CPS}	1577	1397	€/kW
Cost of Balance of Plant	C_{BOP}	25	25	€/kW
Cost of energy storage	C_{STOR*h}	1234	390	€/kW
TCC	**C_{cap}**	2837	1811	**€/kW**
		342	187	**€/kWh**

Table 17
VRFB 1 MW/8.3 MWh and AB-FB 1 MW/9.7 MWh: LCC results.

Parameter	Acronym	Units	VRFB	AB-FB
Variable O&M cost	C_{VOM}	€/kW	0.01	0.01
Annualized Fixed O&M cost	$C_{FOM,a}$	€/kW - year	8.50	8.50
Future cost of replacement	C_R	€/kWh	166.5	131.3
External Environmental cost	C_{EEC}	€	18.16	7.22
Disposal and recycling cost	C_{DR}	€/kW	3.87	6.07
Annualized variable O&M cost	$C_{VOM,a}$	€/kW - year	25.35	34.26
Annualized TCC	$C_{cap,a}$	€/kW - year	21842	13948
Annualized O&M cost	$C_{O\&M,a}$	€/kW - year	33.85	43.12
Annualized Replacement cost	$C_{R,a}$	€/kW - year	5.71E-06	6.01E-06
Annualized Disposal and recycling cost	$C_{DR,a}$	€/kW - year	4.83E-18	7.57E-18
Annualized External Environmental cost	$C_{EEC,a}$	€/kW - year	2.27E-20	9.01E-21
Annualized LCC cost	$C_{LCC,a}$	€/kW - year	21875	13991
Levelized cost of electricity	LCOE	€/kWh	6.45	3.53
Net levelized cost of electricity	LCOS	€/kWh	6.05	3.07

the AB-FB electrolyte. The lack of rebalancing process led to an electricity expenditure of 0.01 kWh/kg of electrolyte for the AB-FB system against 0.04 kWh/kg of electrolyte for the VRFB system. Taking a look at Table 12, the C_{DR} of AB-FB was twice the C_{DR} of VRFB. Even though a rebalancing process was not needed for the AB-FB electrolyte, due to its higher volume (9 times higher than the VRFB's one) the final electricity expenditure for AB-FB was almost the double of VRFB's one. In any case, the $C_{DR,a}$ was practically 0 for both systems (it is not indicated in the table), due to the nature of the calculations (Table 12). Breakdown of the costs can be found in the SI.

C_{EEC} was higher for VRFB than for AB-FB, as expected from the LCA results for the AB-FB system operating as RS wind application. Costs of each impact can be found in the SI. As happened in $C_{DR,a}$, $C_{EEC,a}$ was practically 0 for both systems, due to the nature of the calculations (see Table 12). Regarding the breakdown of the environmental externalities costs (see Fig. 11), the highest contribution came from the TAP, which made sense as its ECF was ranking the highest value on the list (see Table 13), so even if the contribution was low, the cost would be high. GWP contribution was higher in the case of AB-FB, as this value was linked to the water consumption and AB-FB technology involved a larger amount of electrolyte. The rest of the EI values were negligible.

The final step for the LCC was the calculation of $C_{LCC,a}$. Something that can be clearly deduced from the results in Table 17 was the dependence of $C_{LCC,a}$ on $C_{cap,a}$, and thereof in TCC. This made sense, as the nature of the formulae (Table 12) led to this type of result. In any case, the results suggested a more economic scenario when AB-FB

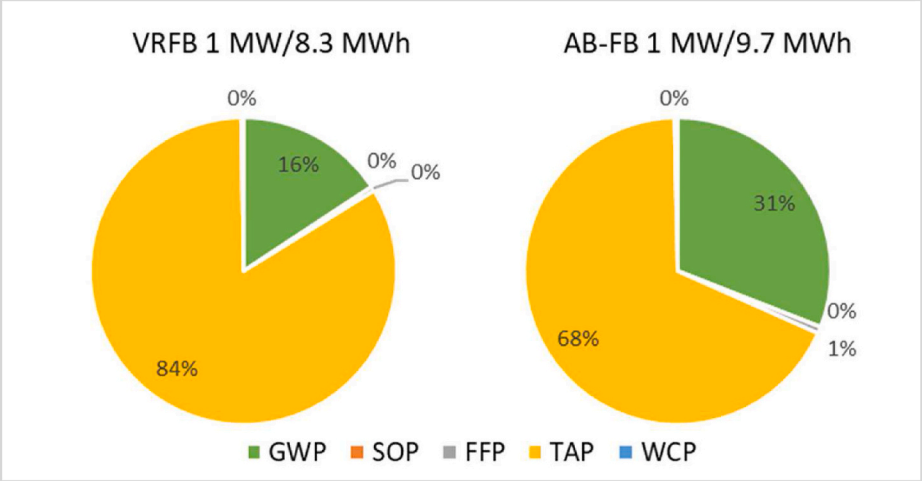

Fig. 11. Environmental Externality Cost for RS wind application. Breakdown of the EIs.

technology was implemented. In this way the LCOE of the AB-FB would be around 3.5 €/kWh (2 times lower than VRFB). LCOS should be used when a global comparison is necessary. In this way the same conclusion applied: AB-FB would be more economic than VRFB. The results were directly linked to the higher cost of the electrolyte and gaskets for VRFB, plus the higher expenditure in carbon electrode due to the cell configuration. If we compare the results of this evaluation with other studies available in literature, the LCOS of the AB-FB is in the range of other RFBs. Even though there is a high variability in the results depending on the type of electrolyte, size, process scenario, among other factors. Most of the found results reported in literature fall between 175 €/MWh and 675 €/MWh (Pawel, 2014; Rodby et al., 2020; Sing Lai and McCulloch, n.d.; Viswanathan et al., 2012). This fact corroborates that the AF-BF technology is a more environmentally clean alternative without implying a significant increase in economic costs with respect to the existing alternatives.

4. Conclusions

In this research, key environmental and economic aspects of an innovative AB-FB technology have been assessed and compared with one VRFB system, which was considered for benchmarking purposes. In addition, valuable information to establish a baseline for the future AB-FB development has been elucidated.

In general, the AB-FB system attained the best environmental performance. O&M was identified as the battery process stage that mostly contributed to the total environmental impact of the battery due to the electricity losses generated during the battery service to support Wind and PV installations. Manufacturing was the second contributing stage, basically, due to the power subsystem components. Generally, the key materials affecting the environmental tendencies were steel, copper, polyethylene and polyvinylchloride required to produce the AB-FB components.

As expected, one of the main advantages of the AB-FB system is related to the electrolyte implications. Compared to the VRFB vanadium-based electrolyte, the AB-FB electrolytic solution is composed by water and salts as main components, which results into a safer and more sustainable technology than the VRFB system. The vanadium-based electrolyte was also responsible of the main VRFB system constrains in terms of costs. According to the applied methodology, the VRFB investment cost (339 €/kWh) was almost twice the AB-FB one (184 €/kWh). It was mostly attributed to the relevance of the energy subsystem cost and, particularly, the VRFB electrolyte production cost, to the total cost of the VRFB technology. Besides the substantial costing differences resulted by the electrolyte production, it was also denoted contribution of the gaskets and the larger amount of carbon electrode used in the VRFB system in comparison with those materials in the AB-FB system. Nevertheless, power subsystem costs were very similar for both ESS. The investment costs were also the key cost drivers when calculating the Net Levelized Cost of Storage, which was 6.05 €/kWh for the AB-FB system in contrast to 3.07 €/kWh for the VRFB system. In this way, the AB-FB technology was determined to be the most economic option.

Results have also highlighted that the AB-FB system service provide benefits to mitigate renewables intermittency, particularly for wind power support. Furthermore, this work has provided insights on what aspects should be addressed to make the AB-FB system even more sustainable from an environmental point of view, and more affordable from an economic point of view. On the one hand, research lines should be focused on improving the efficiency of the battery in order to minimize energy losses during renewable support operation. On the other hand, efforts should be addressed on finding innovative materials to the membranes and reducing consumption of steel and plastic required for the battery component manufacturing by applying circular economy actions, for instance, the use of recycled materials.

CRediT authorship contribution statement

Maryori C. Díaz-Ramírez: Conceptualization, Methodology, Formal analysis, Writing – original draft, Writing – review & editing, Funding acquisition. **Maria Blecua-de-Pedro:** Conceptualization, Methodology, Formal analysis, Writing – original draft, Writing – review & editing, Funding acquisition. **Alvaro J. Arnal:** Conceptualization, Methodology, Formal analysis, Writing – original draft, Writing – review & editing, Funding acquisition. **Jan Post:** Conceptualization, Writing – original draft, Writing – review & editing, Funding acquisition, All authors have read and agreed to the published version of the manuscript.

Declaration of competing interest

The authors declare that they have no known competing financial interests or personal relationships that could have appeared to influence the work reported in this paper.

Acknowledgements

This work was performed in the framework of the BAoBaB project (Blue Acid/Base Battery: Storage and recovery of renewable electrical energy by reversible salt water dissociation). The BAoBaB project has received funding from the European Union's Horizon 2020 Research

and Innovation program under Grant Agreement no. 731187 (www.baobabproject.eu).

The authors also want to thank the support and collaboration of the Centro para el Desarrollo Tecnológico Industrial, E.P.E. (CDTI) funds through the RED CERVERA CER-20191006 “"ALMAGRID: Integración de tecnologías avanzadas de Almacenamiento de Energía para aplicaciones de red”.

The authors also express their gratitude to the AquaBattery BV team due to his support on the AB-FB data gathering process.

Appendix A. Supplementary data

Supplementary data to this article can be found online at https://doi.org/10.1016/j.jclepro.2021.129529.

References

Amelang, S. and Wehrmann, B., 2020 German onshore wind power – output, business and perspectives. https://www.cleanenergywire.org/factsheets/german-onshore-wind-power-output-business-and-perspectives (Accessed 15 February 2021).

Bare, J.C., Gloria, T.P., 2006. Critical analysis of the mathematical relationships and comprehensiveness of life cycle impact assessment approaches. Environ. Sci. Technol. 40, 1104–1113.

Barringer, H.P., Barringer, H.P., 2003. A life cycle cost summary. In: International Conference of Maintenance Societies, pp. 1–10 (ICOMS – 2003).

Battke, B., Schmidt, T.S., Grosspietsch, D., Hoffmann, V.H., 2013. A review and probabilistic model of lifecycle costs of stationary batteries in multiple applications. Renew. Sustain. Energy Rev. 25, 240–250. https://doi.org/10.1016/j.rser.2013.04.023.

Baumann, M., Peters, J.F., Weil, M., Grunwald, A., 2017. CO 2 footprint and life-cycle costs of electrochemical energy storage for stationary grid applications. Energy Technol. 5, 1071–1083. https://doi.org/10.1002/ente.201600622.

Bhattacharjee, A., Roy, A., Banerjee, N., Patra, S., Saha, H., 2018. Precision dynamic equivalent circuit model of a Vanadium Redox Flow Battery and determination of circuit parameters for its optimal performance in renewable energy applications. J. Power Sources 396, 506–518. https://doi.org/10.1016/j.jpowsour.2018.06.017.

Chen, H., Cong, N., Yang, W., Tan, C., Li, Y., Ding, Y., 2009. Progress in electrical energy storage system: a critical review. Prog. Nat. Sci. 19, 291–312. https://doi.org/10.1016/j.pnsc.2008.07.014.

Coester, A., Hofkes, M.W., Papyrakis, E., 2020. Economic analysis of batteries: impact on security of electricity supply and renewable energy expansion in Germany. Appl. Energy 275. https://doi.org/10.1016/j.apenergy.2020.115364.

Culcasi, A., Gurreri, L., Zaffora, A., Cosenza, A., Tamburini, A., Micale, G., 2020. On the modelling of an Acid/Base Flow Battery: an innovative electrical energy storage device based on pH and salinity gradients. Appl. Energy 277, 115576. https://doi.org/10.1016/j.apenergy.2020.115576.

De Bruyn, S., Ahdour, S., Bijleveld, M., De Graaff, L., Schep, E., Schroten, A., Vergeer, R., 2018. Environmental Prices Handbook 2017. Methods and Numbers for Valuation of Environmental Impacts. https://cedelft.eu/wp-content/uploads/sites/2/2021/03/CE_Delft_7N54_Environmental_Prices_Handbook_2017_FINAL.pdf.

De Nocker, L.; Debacker, W. Annex: Monetisation of the MMG Method; OVAM: Mechelen, Belgium, 2018. https://ovam.be/sites/default/files/atoms/files/Monetisation%20of%20the%20MMG%20method%20-%20Anex%20-%20update%202017.pdf (Accessed 15 February 2021).

Díaz-Ramírez, M.C., Ferreira, V.J., García-Armingol, T., López-Sabirón, A.M., Ferreira, G., 2020a. Battery manufacturing resource assessment to minimise component production environmental impacts. Sustainability 12, 6840. https://doi.org/10.3390/su12176840.

Díaz-Ramírez, M.C., Ferreira, V.J., García-Armingol, T., López-Sabirón, A.M., Ferreira, G., 2020b. Environmental assessment of electrochemical energy storage device manufacturing to identify drivers for attaining goals of sustainable materials 4.0. Sustainability 12, 342. https://doi.org/10.3390/su12010342.

European Commision, 2021. Industry 5.0. Towards a Sustainable, Human-Centric and Resilient European Industry. Brussels.

European Commission, 2020a. Critical Raw Materials Resilience: Charting a Path towards Greater Security and Sustainability, Communication from the Commission to the European Parliament, the Council, the European Economic and Social Comittee and the Comittee of the Regions. Brussels, Belgium.

European Commission, 2020b. Weekly Oil Bulletin (19 October 2020 with taxes). https://ec.europa.eu/energy/observatory/reports/2020_10_19_with_taxes_2022.pdf.

Fan, H., Yip, Y., 2019. Elucidating conductivity-permselectivity tradeoffs in electrodialysis and reverse electrodialysis by structure-property analysis of ion-exchange membranes. J. Membr. Sci. 573, 668–681. https://doi.org/10.1016/j.memsci.2018.11.045.

Fernandez-Marchante, C.M., Millán, M., Medina-Santos, J.I., Lobato, J., 2020. Environmental and preliminary cost assessments of redox flow batteries for renewable energy storage. Energy Technol. 8, 1900914 https://doi.org/10.1002/ente.201900914.

Ferreira, H.L., Garde, R., Fulli, G., Kling, W., Lopes, J.P., 2013. Characterisation of electrical energy storage technologies. Energy 53, 288–298. https://doi.org/10.1016/j.energy.2013.02.037.

Gouveia, J., Mendes, A., Monteiro, R., Mata, T.M., Caetano, N.S., Martins, A.A., 2020a. Life cycle assessment of a vanadium flow battery. In: Energy Reports, pp. 95–101. https://doi.org/10.1016/j.egyr.2019.08.025. Elsevier Ltd.

Gouveia, J.R., Silva, E., Mata, T.M., Mendes, A., Caetano, N.S., Martins, A.A., 2020b. Life cycle assessment of a renewable energy generation system with a vanadium redox flow battery in a NZEB household. Energy Rep. 6, 87–94. https://doi.org/10.1016/j.egyr.2019.08.024.

Ibrahim, H., Ilinca, A., Perron, J., 2008. Energy storage systems—characteristics and comparisons. Renew. Sustain. Energy Rev. 12, 1221–1250. https://doi.org/10.1016/j.rser.2007.01.023.

IEA Wind, 2017. IEA Wind Technology Collaboration Programme 2017 Annual Report. https://iea-wind.org/wp-content/uploads/2020/12/Annual-Report-2017.pdf (Accessed 15 February 2021).

EDP International AB. 2020. Product Category Rule (PCR) 2007:08 Electricity, steam and hot water generation and distribution. Version 4.11. 2020. https://www.environdec.com/pcr-library.

Javed, M.S., Ma, T., Jurasz, J., Canales, F.A., Lin, S., Ahmed, S., Zhang, Y., 2021. Economic analysis and optimization of a renewable energy based power supply system with different energy storages for a remote island. Renew. Energy 164, 1376–1394. https://doi.org/10.1016/j.renene.2020.10.063.

Jülch, V., 2016. Comparison of Electricity Storage Options Using Levelized Cost of Storage (LCOS) Method. https://doi.org/10.1016/j.apenergy.2016.08.165.

Kear, G., Shah, A.A., Walsh, F.C., 2012. Development of the all-vanadium redox flow battery for energy storage: a review of technological, financial and policy aspects. Int. J. Energy Res. 36, 1105–1120. https://doi.org/10.1002/er.1863.

Li, M.J., Zhao, W., Chen, X., Tao, W.Q., 2017. Economic analysis of a new class of vanadium redox-flow battery for medium- and large-scale energy storage in commercial applications with renewable energy. Appl. Therm. Eng. 114, 802–814. https://doi.org/10.1016/j.applthermaleng.2016.11.156.

Longo, S., Antonucci, V., Cellura, M., Ferraro, M., 2013. Life Cycle Assessment of Storage Systems: the Case Study of a Sodium/nickel Chloride Battery. https://doi.org/10.1016/j.jclepro.2013.10.004.

Lopez, S., Akizu-Gardoki, O., Lizundia, E., 2020. Comparative Life Cycle Assessment of High Performance Lithium-Sulfur Battery Cathodes. https://doi.org/10.1016/j.jclepro.2020.124528.

Lourenssen, K., Williams, J., Ahmadpour, F., Clemmer, R., Tasnim, S., 2019. Vanadium redox flow batteries : a comprehensive review. J. Energy Storage 25.

Mcmanus, M.C., 2012. Environmental Consequences of the Use of Batteries in Low Carbon Systems: the Impact of Battery Production. https://doi.org/10.1016/j.apenergy.2011.12.062.

Morales-Mora, M.A., Pijpers, J.J.H., Antonio, A.C., Soto, J.D.L.C., Calderón, A.M.A., 2021. Life cycle assessment of a novel bipolar electrodialysis-based flow battery concept and its potential use to mitigate the intermittency of renewable energy generation. J. Energy Storage 35. https://doi.org/10.1016/j.est.2021.102339.

Noack, J., Wietschel, L., Roznyatovskaya, N., Pinkwart, K., Tübke, J., 2016. Techno-economic modeling and analysis of redox flow battery systems. Energies 9, 627. https://doi.org/10.3390/en9080627.

Norgate, T., 2013. Metal Recycling: the Need for a Life Cycle Approach. EP135565, CSIRO. Australia.

Opatokun, S.A., Lopez-Sabiron, A., Ferreira, G., Strezov, V., 2017. Life cycle analysis of energy production from food waste through anaerobic digestion, pyrolysis and integrated energy system. Sustainability 9, 1804. https://doi.org/10.3390/su9101804.

Pärnamäe, R., Gurreri, L., Post, J., Johannes Van Egmond, W., Culcasi, A., Saakes, M., Cen, J., Goosen, E., Tamburini, A., Vermaas, D.A., Tedesco, M., 2020. Membranes the Acid-Base Flow Battery: Sustainable Energy Storage via Reversible Water Dissociation with Bipolar Membranes. https://doi.org/10.3390/membranes10120409.

Pawel, I., 2014. Selection and peer-review under responsibility of EUROSOLAR-The European Association for Renewable Energy the cost of storage-how to calculate the levelized cost of stored energy (LCOE) and applications to renewable energy generation. Energy Procedia 46, 68–77. https://doi.org/10.1016/j.egypro.2014.01.159.

Poonpun, P., Jewell, W.T., . Analysis of the cost per kilowatt hour to store electricity. IEEE Trans. Energy Convers. 23, 529–534. https://doi.org/10.1109/TEC.2007.914157.

Rodby, K.E., Carney, T.J., Ashraf Gandomi, Y., Barton, J.L., Darling, R.M., Brushett, F.R., 2020. Assessing the levelized cost of vanadium redox flow batteries with capacity fade and rebalancing. J. Power Sources 460, 227958. https://doi.org/10.1016/j.jpowsour.2020.227958.

Sánchez-Díez, E., Ventosa, E., Guarnieri, M., Trovò, A., Flox, C., Marcilla, R., Soavi, F., Mazur, P., Aranzabe, E., Ferret, R., 2021. Redox flow batteries: status and perspective towards sustainable stationary energy storage. J. Power Sources 481. https://doi.org/10.1016/j.jpowsour.2020.228804.

Sing Lai, C., McCulloch, M.D., 2017. Levelized cost of electricity for solar photovoltaic and electrical energy storage. https://doi.org/10.1016/j.apenergy.2016.12.153.

Troy, S., Schreiber, A., Reppert, T., Gehrke, H.G., Finsterbusch, M., Uhlenbruck, S., Stenzel, P., 2016. Life Cycle Assessment and resource analysis of all-solid-state batteries. Appl. Energy 169, 757–767. https://doi.org/10.1016/j.apenergy.2016.02.064.

van Egmond, W.J., Saakes, M., Noor, I., Porada, S., Buisman, C.J.N., Hamelers, H.V.M., 2018. Performance of an environmentally benign acid base flow battery at high energy density. Int. J. Energy Res. 42, 1524–1535. https://doi.org/10.1002/er.3941.

Viswanathan, V., Crawford, A., Stephenson, D., Kim, S., Wang, W., Li, B., Coffey, G., Thomsen, E., Graff, G., Balducci, P., Kintner-Meyer, M., Sprenkle, V., 2012. Cost and

Performance Model for Redox Flow Batteries. https://doi.org/10.1016/j.jpowsour.2012.12.023.
Weber, S., Peters, J.F., Baumann, M., Weil, M., 2018. Life cycle assessment of a vanadium redox flow battery. Environ. Sci. Technol. 52, 10864–10873. https://doi.org/10.1021/acs.est.8b02073.
Zakeri, B., Syri, S., 2015. Electrical energy storage systems: a comparative life cycle cost analysis. Renew. Sustain. Energy Rev. 42, 569–596. https://doi.org/10.1016/j.rser.2014.10.011.
Zhang, Y., Hua, Q.S., Sun, L., Liu, Q., 2020. Life cycle optimization of renewable energy systems configuration with hybrid battery/hydrogen storage: a comparative study. J. Energy Storage 30. https://doi.org/10.1016/j.est.2020.101470.